P-03-77

Forsmark site investigation

Dissolution of quartz, vug formation and new grain growth associated with post-metamorphic hydrothermal alteration in KFM02A

C Möller, S Snäll, M B Stephens
Geological Survey of Sweden

Juni 2003

Svensk Kärnbränslehantering AB
Swedish Nuclear Fuel
and Waste Management Co
Box 5864
SE-102 40 Stockholm Sweden
Tel 08-459 84 00
+46 8 459 84 00
Fax 08-661 57 19
+46 8 661 57 19

ISSN 1651-4416
SKB P-03-77

Forsmark site investigation

Dissolution of quartz, vug formation and new grain growth associated with post-metamorphic hydrothermal alteration in KFM02A

C Möller, S Snäll, M B Stephens
Geological Survey of Sweden

Juni 2003

Contents

1 Introduction

As part of the site investigation programme at Forsmark, two cored boreholes (KFM01A and KFM02A) have been drilled down to a depth of c 1,000 m at two separate localities in the Forsmark candidate area (Figure 1-1). At the time of writing of this report, a third cored borehole (KFM03A) is in the process of being drilled at a third locality (Figure 1-1). In drillcore KFM02A, zones of strongly altered, reddened metagranite with abundant vugs were encountered at 175, 180 and 250–300 m depth. Strongly altered amphibolite as well as pegmatite and finer-grained metagranitoid with similar cavities are also present. Furthermore, a several decimeter wide section in the lower part of the 250–300 m depth interval is altered and fractured to such an extent that the bedrock has lost its coherence (Figure 1-2). Since metagranite with vugs displays low strength, may potentially be more permeable in character than the metagranite which is devoid of vugs and may even host ore minerals (e.g. U, Sn-W-Mo, Au, Pb-Zn-Cu), it was judged necessary to initiate a special investigation of the anomalous, strongly altered bedrock in KFM02A.

Figure 1-1. *Location of boreholes KFM01A, KFM02A and KFM03A in the Forsmark candidate area.*

Figure 1-2. *Photographs of the KFM02A drillcore showing well-preserved (a, upper picture) and strongly altered (b, lower picture) metagranite. Note the incoherent section in amphibolite at c 291.0–291.5 m. Photographs taken by Alf Sevastik.*

2 Regional geological setting

Bedrock mapping at the surface /Stephens et al, 2003/ has shown that the Forsmark candidate area is dominated by medium-grained granite with mafic enclaves and dykes; a medium-grained granodiorite to tonalite body is prominent in the southeastern part of the candidate area. All these rocks were metamorphosed under amphibolite-facies conditions and affected by penetrative ductile deformation after c 1,880 million years ago. Younger dykes and minor intrusions of finer-grained granodiorite, tonalite and granite as well as pegmatite and granite, which are all variably affected by ductile deformation and metamorphism, form volumetrically subordinate rock components. The age and affinity of these minor intrusions are uncertain. Major intrusions of younger granite are only exposed several tens of kilometres to the south and west of the candidate area, for example in the Mälaren area. These granites formed c 1,800 million years ago and, at least locally, are characterized by distinctive U and Th anomalies.

The Forsmark candidate area is situated in the segment of the Fennoscandian Shield /Koistinen et al, 2001/ where early crustal-building and crustal-reworking phases were completed by c 1,750 million years ago /SKB, 2002/. Furthermore, by c 1,750–1,700 million years ago, this part of the shield had cooled and stabilized sufficiently such that the deformational régime had become more brittle in character. Nevertheless, important pulses of intrusive activity at high crustal levels are an important feature of the later geological history in central Sweden, Åland and southwest Finland.

Intrusion of granites and extensive volcanism affected the western part of central Sweden during the latest part of the Palaeoproterozoic, c 1,710 to 1,660 million years ago. Intrusion of rapakivi granites as well as dolerite and porphyry dykes occurred c 1,590, 1,500 and 1,470 million years ago in central Sweden, on Åland and in southwest Finland. Dolerite sills and dykes intruded the crust in these areas c 250 million years later. Subsidence and sedimentation also characterized certain time-periods after c 1,700 million years ago /SKB, 2002/. It is probable that all this activity had an important influence on the thermal régime in the bedrock of central Sweden and, by consequence, the circulation of hydrothermal fluids.

3 Objective and scope

The main purpose of the present study has been to document the mineralogical, textural and microstructural character of the altered rocks in the depth interval 250–300 m in borehole KFM02A, and to investigate whether they contain any mineralisation with potentially economic interest. It was decided, at this stage in the investigations, to focus attention on representative unaltered rocks, altered rocks and mineral infillings in the vugs, with the help of optical microscopy, electron microscopy, energi-dispersive X-ray (EDX) analysis connected to an electron microscope, and standard X-ray diffraction (XRD) analysis.

A second aim has been to shed some light on the processes which have given rise to the vuggy metagranite and associated rocks. Vugs in igneous rocks can form by widely different processes. They may have a magmatic origin (entrapment of gas bubbles), a deep-seated subsolidus origin (fluid-controlled dissolution processes under late-stage magmatic or various post-magmatic conditions), or may have formed as a result of weathering. The present study includes a review of published studies relevant for comparison with the porous rocks in drillcore KFM02A. The review provides some insight into the processes responsible for vug formation and associated mineral precipitation in the metagranite and associated rocks, and leads to some suggestions for further studies.

4 Equipment

Optical microscopic investigations were made using a standard polarizing microscope at the Geological Survey of Sweden (regional office, Lund).

Photomicrographs were taken using a polarizing microscope with digital photographic equipment at the Department of Geology, University of Lund. Leif Johansson kindly provided access to and assistance with the use of the digital photographic and scanning equipment at the University of Lund. Thin-section overview images were prepared using digital scanning equipment at the same institution. Digital photographs and scanned images of thin-sections were processed using Adobe Photoshop Elements 2.0 software.

Electron microscopy, mineral identification and semi-quantitative mineral analysis were made by EDX analysis connected to a Jeol electron microscope at the Department of Geology, University of Lund.

XRD work was carried out at the mineralogical laboratory at the Geological Survey of Sweden (head office, Uppsala) using a Siemens D5000 (theta-theta) diffractometer.

5 Execution

At the end of January 2003, eight small batches of material, primarily scraped from vugs and fracture fillings, were sampled from the 250–300 m depth interval for mineral identification using XRD analysis. A first set of seven samples from both unaltered and altered rocks at the same level were also taken from the KFM02A drillcore for thin-section preparation. Minoprep (Hunnebostrand, Sweden) prepared eight thin-sections. Sampling work at this stage was carried out by Jenny Andersson (activity leader for geology, Forsmark).

A literature search and a compilation of relevant data from published literature were initiated at the end of February. This work was carried out more or less at the same time as optical microscopic studies that aimed to document the mineralogical, textural and microstructural character of the altered and unaltered rocks within and close to the 250–300 m depth interval. The first set of samples was also analysed with the help of the XRD technique.

On-site inspection of the drillcore was carried out during late March and a complementary round of sampling was completed for optical microscopic, scanning electron microscopic (SEM) and XRD work. Five new samples for thin-section preparation, four new samples for XRD analysis and one sample for SEM work were selected. One of the samples for thin-section preparation was taken from a vuggy, fine-grained metagranitoid at the 175 m level. Five samples were also taken for whole-rock geochemistry and five samples for petrophysical investigations within and close to the 250–300 m depth interval. Such analyses do not form part of the present study but need to be carried out in a follow-up study. On-site inspection of the drillcore and sampling were carried out by Andersson, Möller, Snäll and Stephens.

Subsequent work during late March and April involved the digital scanning of thin-sections and production of the first set of digital photographs. These images were used for textural and microstructural interpretation and as “maps” during electron microscopy and EDX analysis which were completed during mid-April. Special care was taken to identify heavy minerals that occur in abundance in the altered metagranite. The second set of thin-sections was obtained from Minoprep during the early part of April. Inspection of these thin-sections as well as digital scanning and image preparation were subsequently completed and scanned images of thin-sections were processed. The second batch of XRD analyses was also carried out on the complementary samples from the 250–300 m depth interval.

EDX analysis was carried out on three thin-sections which were coated with carbon. Operating conditions during EDX analysis were 18 kV accelerating voltage with a standard beam current of 2.5 nA and a counting time of 100 s. The routine analytical set-up TEM97F was used. This covers the elements Si, Ti, Al, Fe, Mn, Mg, Ca, Na and K. The equipment utilises Link’s software for ZAF-correction and data processing, with natural and synthetic mineral standards. The beam size (3 micrometers) allows analysis of minerals with grain-sizes down to a radius of c 5 micrometers.

Each analysis contains the elements identified in the spectrum (above 2σ level), with amounts calculated by the Link analytical system as weight-% oxides and in stoichiometric proportions based on a chosen number of oxygen atoms in the formula. Fe is assumed to be ferrous in these calculations, with the exception of epidote for which all Fe was

recalculated as ferric. Precision is generally ± 2%. However, Na is especially difficult to analyse since it has low atomic weight and evaporates under the beam. For this reason, plagioclase feldspar analyses are low in Na and totals. The low totals for biotite and chlorite reflect the presence of hydrous components. These components cannot be analysed by electron microprobe techniques.

Most of the samples collected for XRD analysis were scraped from the walls of vugs that occur in the 250–300 m level depth interval. In order to prepare each specimen for powder XRD analysis, the material was ground by hand in an agate mortal. The powder was subsequently placed in a special sample holder for XRD analysis. However, the amounts of material for several samples were too small to fill the sample holder. In such cases, the powder was placed on glass plates and smeared out by dispersion of the powder in alcohol. After drying, the mineral concentrates in the samples were oriented more or less parallel to the surface of the plates, especially the phyllosilicate concentrates. In cases with somewhat larger amounts of material, the samples were placed in a beaker of distilled water in an ultrasonic bath. With the help of the treatment in the ultrasonic bath, the particles that cover the walls of the rock vugs were released into the water. After several minutes treatment in the ultrasonic bath, the water was loaded with suspension particles. Specimens for XRD analysis were prepared from these suspensions according to /Drever, 1973/.

The radiation (CuK_{α}) in the diffractometer was generated at 40 kV and 40 mA, and the X-rays were focussed with a graphite monochromator. Scans were run from 2°–65° (2-theta) or from 2°–35° (samples with preferred crystal orientation) with step size 0.02° (2-theta) and counting time 1 s $step^{-1}$. The analyses were performed with a fixed 1° divergence and a 2 mm receiving slit. The XRD raw files were taken up in the Bruker/ Siemens $DIFFRAC^{PLUS}$ software (version 2.2), and evaluated in the programme EVA. The minerals were identified by means of the /PDF, 1994/ computer database. The best-fit identification line chosen for plagioclase feldspar and displayed on the various figures below is albite.

Thomas Eliasson (Geological Survey of Sweden) and Jesper Petersson (SwedPower AB) kindly reviewed earlier drafts of the manuscript and contributed with suggestions for improvements.

6 Results

6.1 Vuggy metagranite and altered amphibolite in drillcore KFM02A

Reconnaisance mapping of borehole KFM02A shows that the type and relative frequency of the different rock types in the borehole are similar to that observed at the surface. Medium-grained metagranite is dominant; fine-grained metagranitoid, amphibolite and pegmatite are subordinate components. With the exception of more fractured bedrock at two sites in the depth interval c 400–500 m and at c 900 m depth, there is a concentration of fractures in the upper 300 m. The mapping also indicates that, with the exception of the depth intervals 175, 180 and 250–300 m, the rocks completely lack or display only faint to weak alteration.

A summary of the mineralogical, textural and microstructural characteristics of unaltered metagranite, altered metagranite with vugs and altered amphibolite, predominantly from the 250–300 m depth interval, is presented below. Detailed descriptions of individual thin-sections are provided in Appendix A. Mineral compositions reported in this section rely on the semi-quantitative EDX analyses and the XRD analyses reported in sections 6.1.2 and 6.1.3, respectively.

6.1.1 Mineralogical, textural and microstructural characteristics of unaltered and altered rocks

Unaltered metagranite

The unaltered or weakly altered rocks have a ductile deformational fabric (lineation-L, foliation-S or a combined L-S fabric) that is clearly visible in hand specimen and defined by elongate quartz and feldspar domains as well as oriented biotite grains (Figure 6-1a). Thin-sections reveal a recrystallised, generally finer-grained fabric than the medium-grained appearance of the rock. Individual mineral grains vary in size from < 0.5 to c 3 mm.

The mineral assemblages in the unaltered metagranite are characteristic for amphibolite-facies metamorphic conditions at temperatures beneath that necessary for anatexis. Minerals include K-feldspar (with exsolved albite-lamellae), plagioclase feldspar with an oligoclase composition, quartz, biotite and epidote (Figure 6-1b). Accessory minerals are apatite, zircon and, in small amounts, allanite and magnetite. Late alteration is moderate or, in the best preserved rocks, local and includes staining of plagioclase and replacement of biotite by chlorite, epidote and pumpellyite (Figure 6-1b).

Much of the strong ductile deformational fabric has developed at high temperatures, under amphibolite-facies metamorphic conditions. At such temperatures (> 550°C), strain is accommodated by recrystallisation. However, some intracrystalline strain features are also present. Feldspars commonly show slight bending or kinking of the lattice. Quartz shows undulose extinction and deformation lamellae, and has sutured grain-boundaries (Figure 6-1c), the latter demonstrating recrystallisation by grain-boundary migration. This deformation presumably occurred during later, retrograde metamorphic conditions.

Figure 6-1. *Thin-section photomicrographs of unaltered metagranite (sample KFM02A, 317.26 m, A2 in Appendix A). Abbreviations in Figures 6-1, 6-2, 6-3 and 6-4 are Alb = albite, Ap = apatite, Bi = biotite, Chl = chlorite, Ep = epidote, Hem = hematite, Kfsp = K-feldspar, Pl = plagioclase feldspar, Pump = pumpellyite, Qz = quartz, Ti-ox = Ti- oxide, Zr = zircon.*

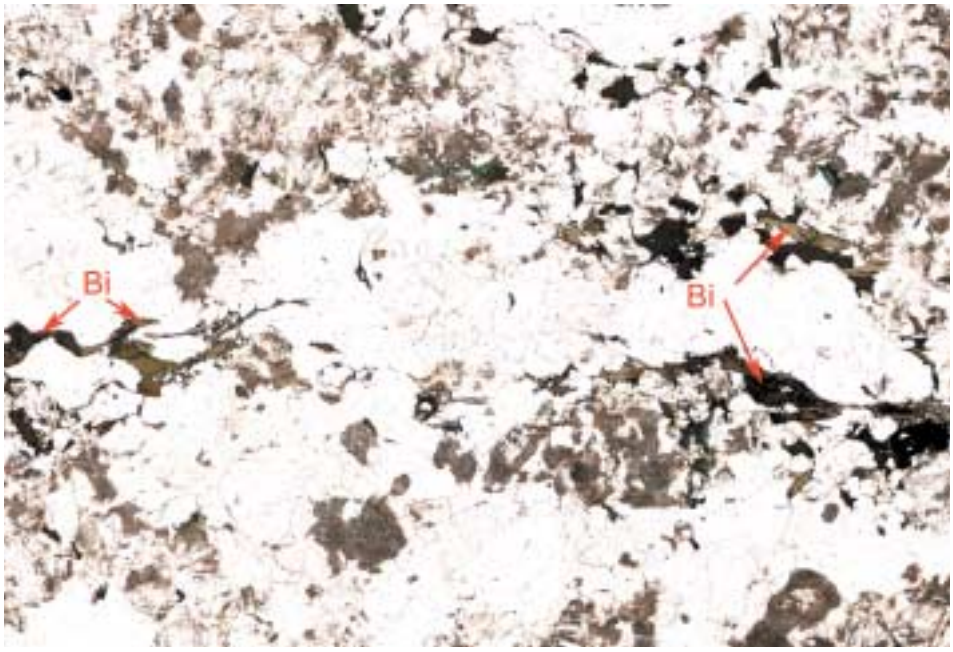

a) Ductile deformational fabric defined by elongate quartz domains (clear, 2–3 mm thick areas), feldspar domains (plagioclase feldspar, partly with a "dusty" or "stained" appearance), and oriented grains of biotite. Width of view = 17 mm.

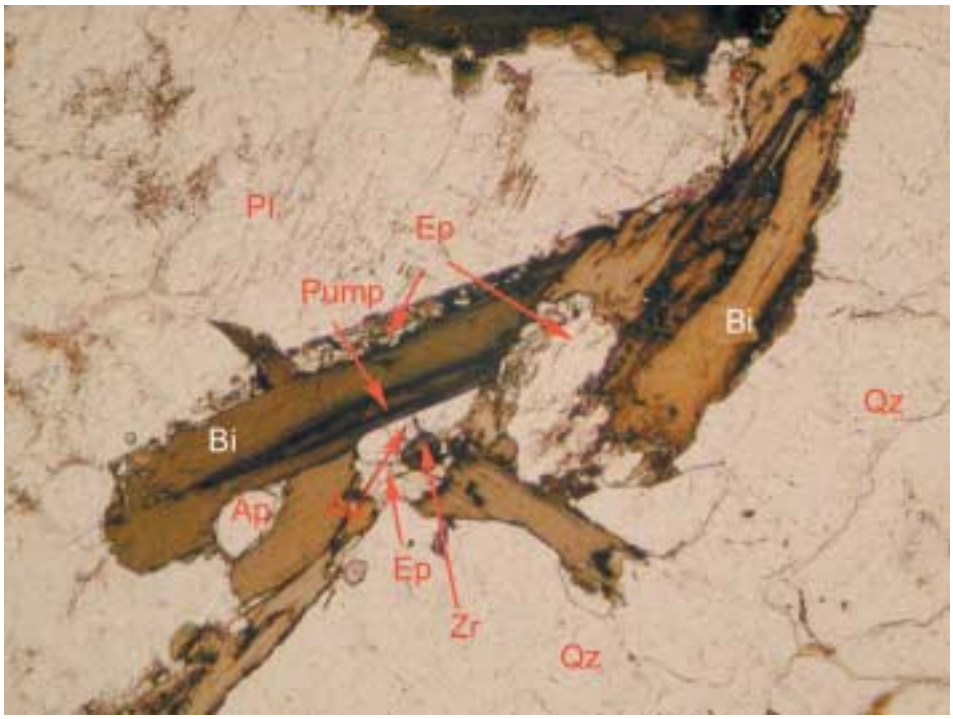

b) Biotite with spool-shaped lamellae of pumpellyite, and rimmed by fine grains of epidote. Zircon and apatite are also present. Width of view = 1.8 mm.

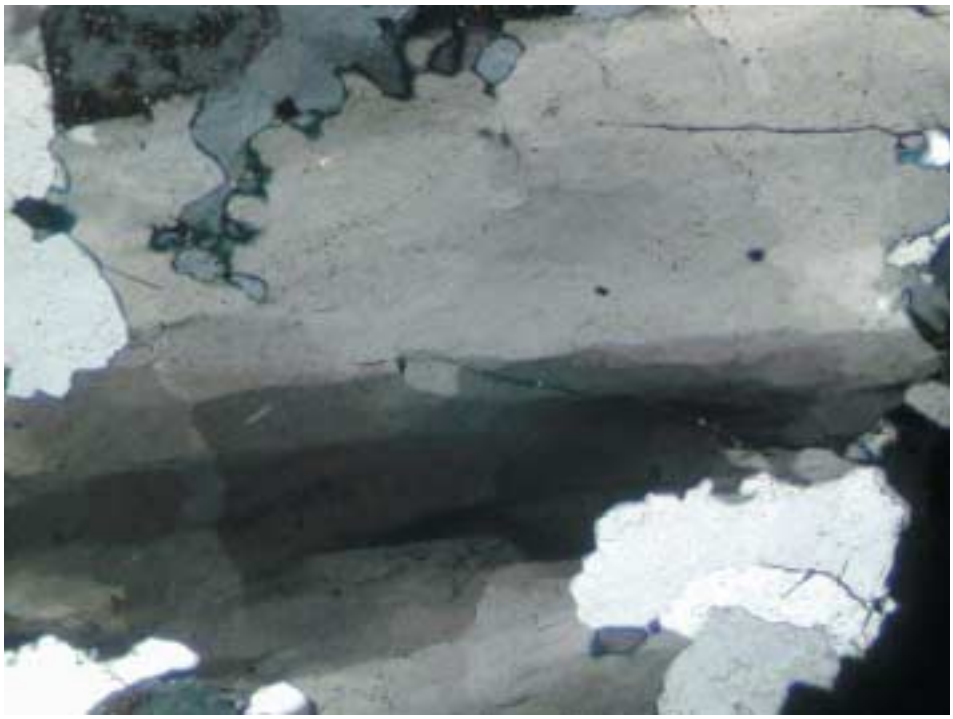

c) Quartz domain (cross-polarised light) with features typical for recrystallisation by grain-boundary migration. A large, strained grain with undulous extinction in the centre of the picture is bounded by sutured grain boundaries towards surrounding, irregularly shaped and less strained grains. Width of view = 1.8 mm.

Altered metagranite with vugs

In drillcore KFM02A, alteration and formation of vugs has been encountered in two types of metagranitoid, the dominant medium-grained metagranite and a subordinate, fine-grained metagranitoid. With the exception of the resilicified varieties (see below), the altered rocks are deficient in quartz and dominantly composed of a porous framework of feldspars (Figure 6-2a). The plagioclase feldspar grains are heavily stained with minute grains of Fe-oxide and sericite, and have abundant tiny pits (Figure 6-2b). The rims of individual plagioclase feldspar grains are often clear adjacent to the vugs. The composition of the original plagioclase feldspar has been completely altered to albite. K-feldspar grains are clear but often have embayed and resorbed rims. Biotite has been altered to a virtually opaque mass (Figures 6-2c and d) which consists of chlorite, tiny hematite grains and aggregates of Ti-oxide grains (probably anatase, possibly rutile, usually 5–15 micrometers large grains). Apatite and zircon are commonly present together with the biotite pseudomorphs, in the same textural position as in the unaltered metagranite. Apatite appears unaffected by alteration. By contrast, zircon is commonly partly altered (see analytical results below). Single, small grains of Fe-sulphide are also present.

Figure 6-2. *Thin-section photomicrographs and back-scatter electron (BSE) images illustrating alteration features in metagranite (sample KFM02A, 295.87–295.89 m, D1 in Appendix A). Abbreviations are listed under Figure 6-1, above.*

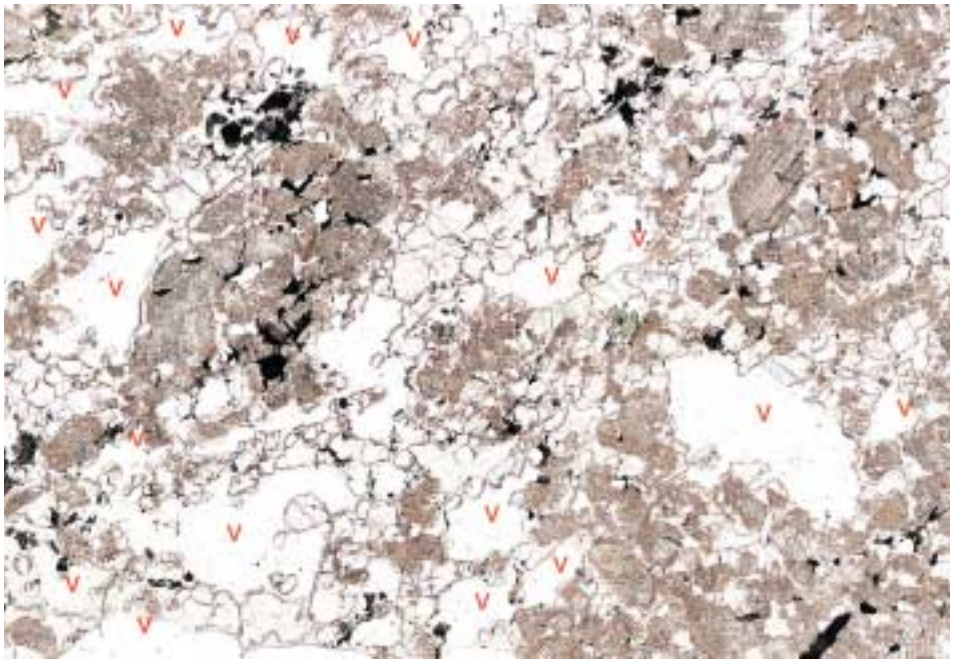

a) Overview of feldspar "framework" and vugs (all but the smallest are marked with a "v"). Plagioclase feldspar has a strongly stained appearance but commonly displays a clear rim immediately adjacent to a vug. K-feldspar is clear and colourless. Width of view = c 20 mm.

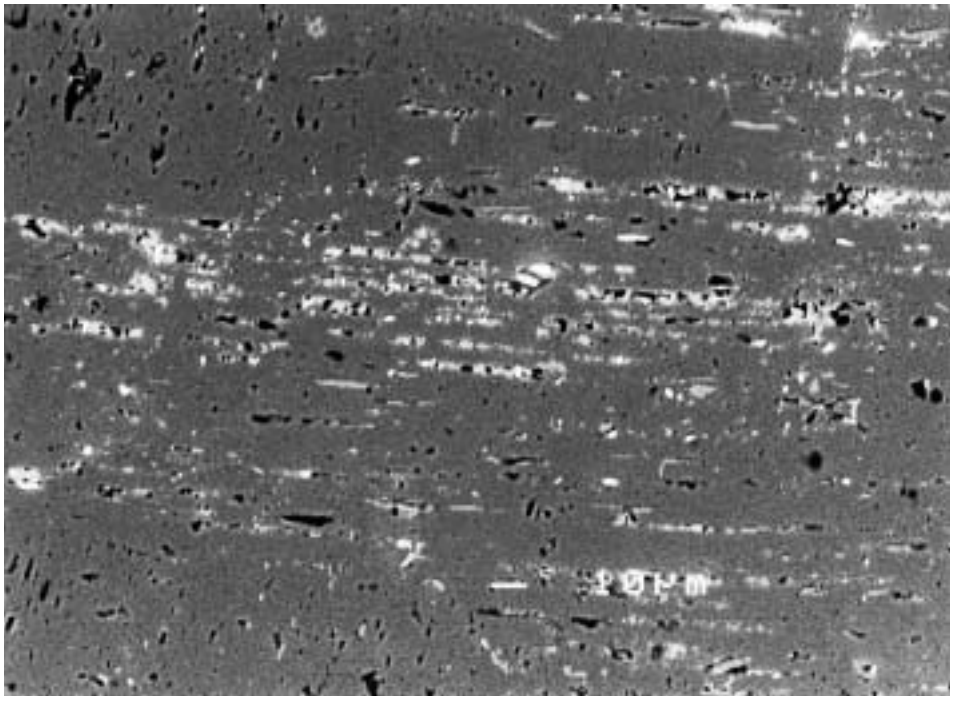

b) BSE image of stained plagioclase feldspar (medium grey, altered to pure albite), with minute grains of Fe-oxide (brightest spots), sericite (light) and frequent small pits (black). Scale bar = 10 micrometers.

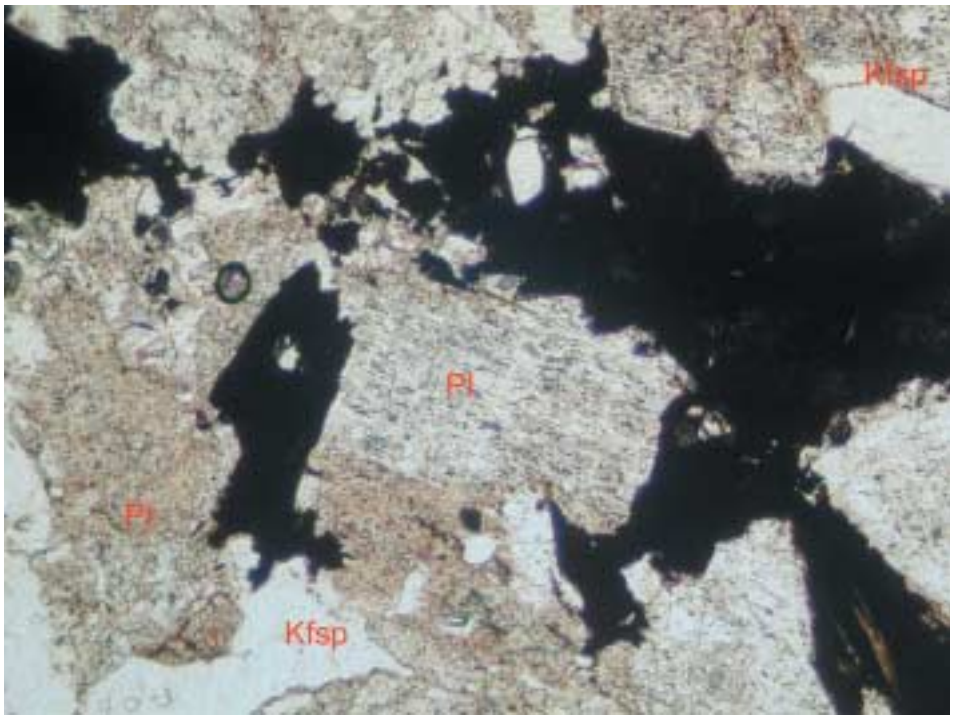

c) Opaque-looking pseudomorphs after biotite. Width of view = 1.8 mm.

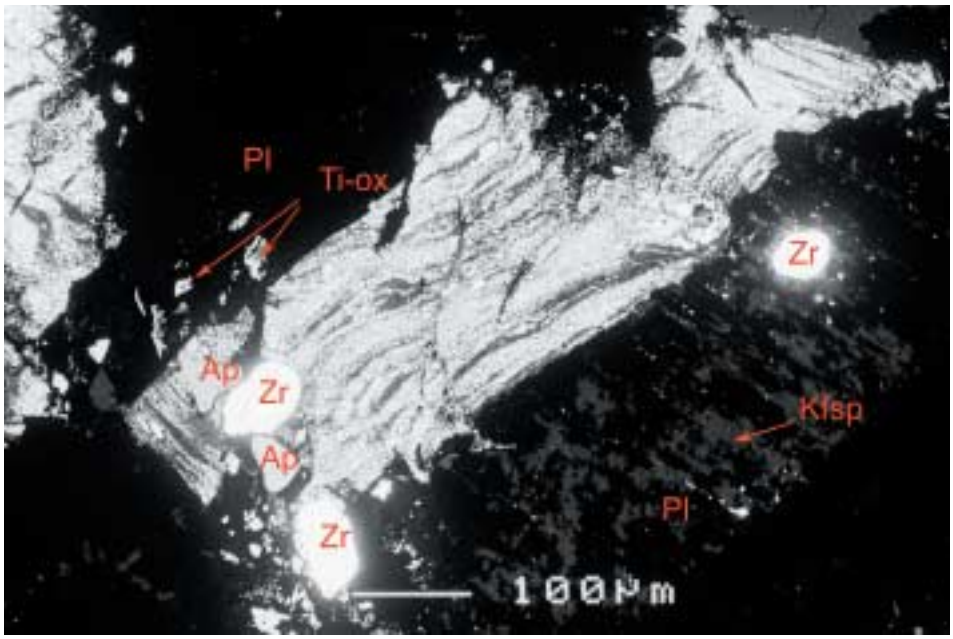

d) BSE image of pseudomorph (bright-spotted mineral) after biotite, consisting of hematite (bright, individual grains < 5 micrometers large) intergrown with chlorite (dark). The biotite pseudomorph is surrounded by albitised plagioclase feldspar (dark). The plagioclase feldspar in the lower right part of the picture contains K-feldspar intergrowths (dark grey). Within and adjacent to the pseudomorph, bright grains of Ti-oxide (probably anatase) occur. Zircon and apatite are also present. Scale bar = 0.1 mm.

Vugs are present irrespective of whether the metagranite has a moderately or strongly (Figure 6-3a) developed ductile deformational fabric. The vugs are open spaces into which original feldspars project and within which new, strain-free, often idiomorphic crystals of albite and quartz have precipitated (Figures 6-3b and c). Very thin, fine-grained, colourless fringes, which consist of K-feldspar and albite, occur on the resorbed rims of the original feldspars. The K-feldspar in these rims is rugged in shape, hollow and most probably represents the resorbed rims of original K-feldspar grains (Figures 6-3c and d). By contrast, albite forms small idiomorphic crystals that are clearly newly precipitated. Tiny (< 1 micrometer) grains of hematite usually occur in the K-feldspar grains along the boundary to the resorbed rim. Radial aggregates of chlorite, commonly heavily stained by hematite, occur in the vugs (Figure 6-3e). Small grains of Ti-oxide are present locally within these aggregates.

Figure 6-3. *Thin section photomicrographs and BSE images illustrating the vugs in altered metagranite. With the exception of Figure 6-3a, the photomicrographs are from sample KFM02A, 295.87–295.89 m (D2 in Appendix A.) Abbreviations are listed under Figure 6-1, above.*

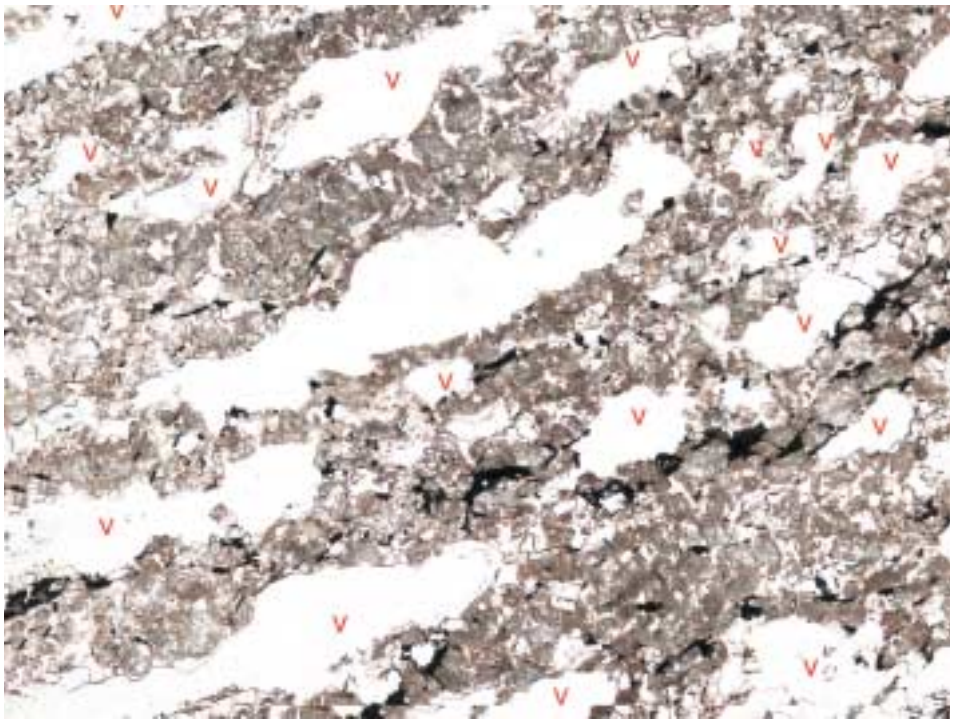

a) Overview showing vugs (marked "v") developed in metagranite with a strong ductile deformational fabric (sample KFM02A, 290.25–290.28 m, D3 in Appendix A). Plagioclase feldspar has a strongly stained appearance. K-feldspar is clear and colourless. Width of view = c 20 mm.

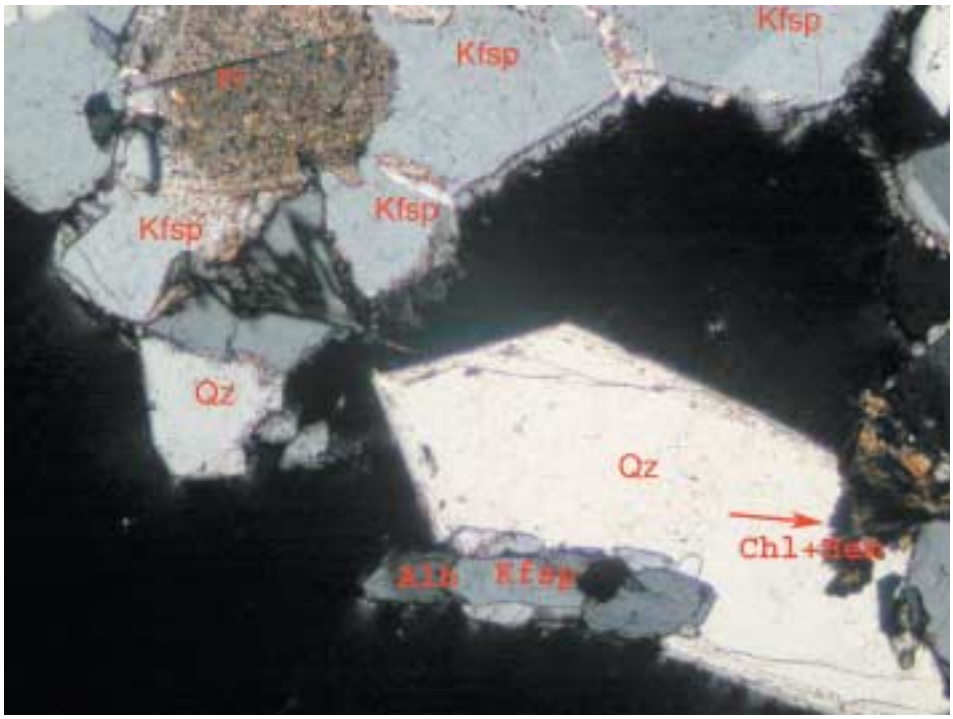

b) Photomicrograph (cross-polarised light) showing a sectioned vug wall (black = cavity). The "original" plagioclase (upper left) is stained and albitised and there are irregular albite lamellae (white) in K-feldspar. Thin rims occur along the "old" feldspar grains. New, idiomorphic quartz and albite crystals project into the vugs. Width of view = 1.8 mm.

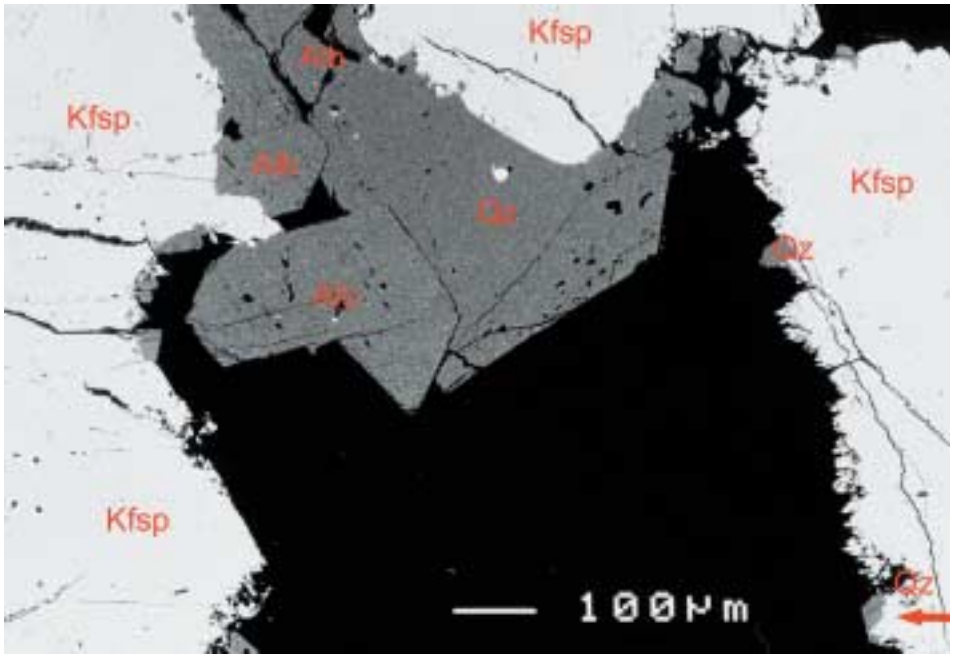

c) BSE image showing idiomorphic crystals of albite and quartz (medium grey) on a sectioned vug wall (black = cavity). The thin rims (cf Figure 6-2b) on K-feldspar grains (light grey) along the vug walls are irregular fringes of K-feldspar and small euhedral crystals of albite and quartz. Scale bar = 0.1 mm.

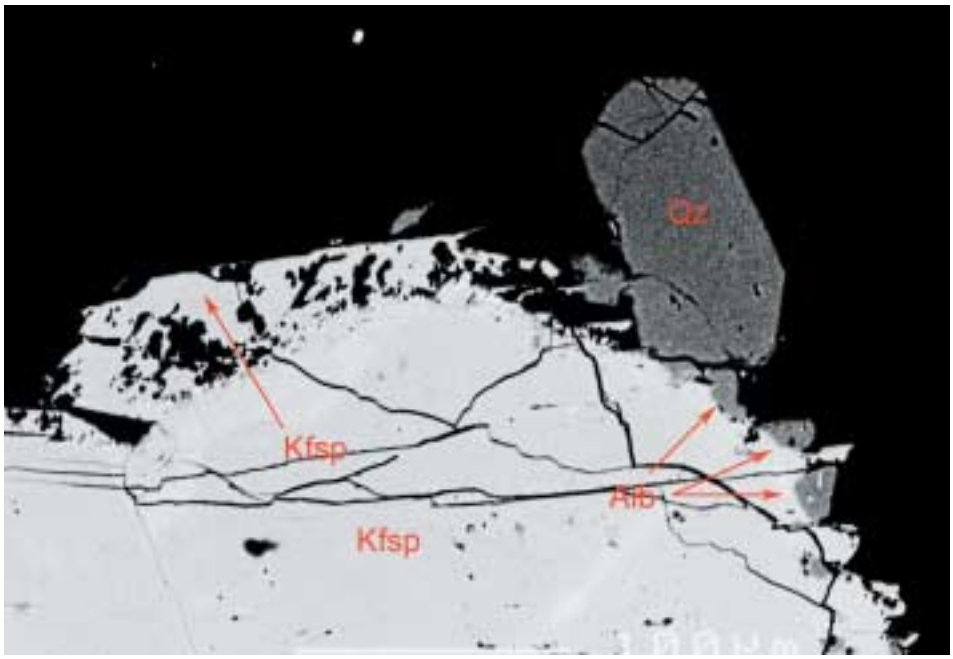

d) Detailed BSE image of a thin felsic rim on a K-feldspar grain. The photomicrograph shows the rugged shapes of the K-feldspar fringes (light grey) and the idiomorphic shapes of albite and quartz grains (both medium grey). Black = cavity. Scale bar = 0.1 mm.

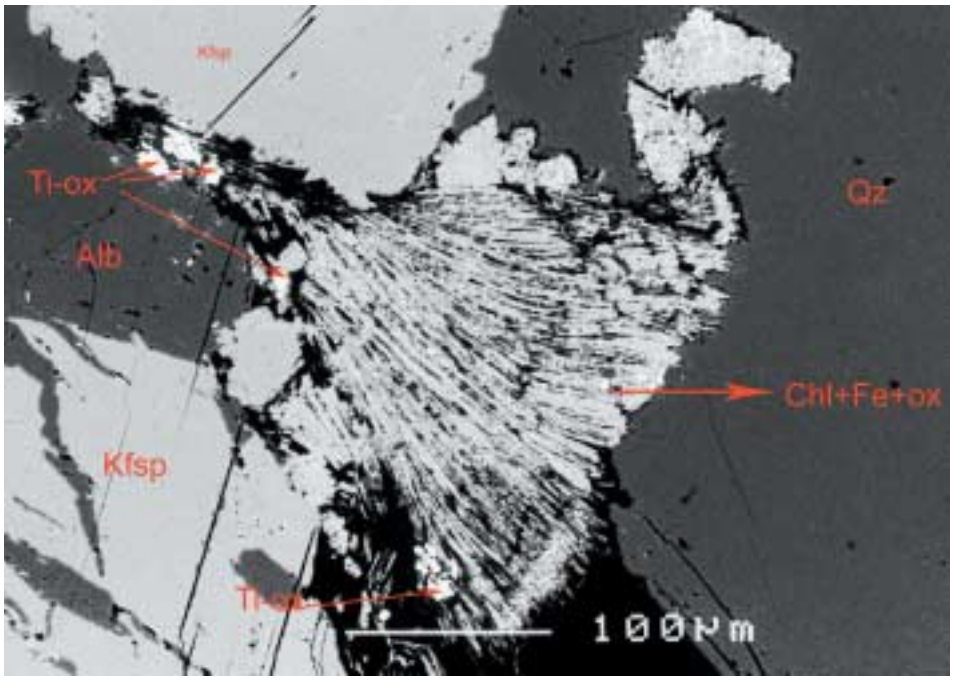

e) BSE image illustrating chlorite + hematite aggregate (bright-spotted aggregate in the centre) on a vug wall. Small grains of Ti-oxide (bright) and, in the right-hand part of the picture, a large quartz crystal (medium grey) are also present. The vug wall (left-hand part of the photomicrograph) consists of K-feldspar (light grey) and albitised plagioclase feldspar (medium grey). Black = cavity (central lower part of the photomicrograph). Scale bar = 0.1 mm.

Idiomorphic quartz appears as the latest crystallised phase in almost all samples of altered metagranite. In places, quartz has overgrown the fine fringes and, locally, quartz completely fills the former vugs. In some samples, the secondary quartz carries abundant tiny inclusions (e.g. sample B1). In one sample (C3 in Appendix A), a fine coating of colourless minerals with inclusions of hematite and chlorite was found on the crystal faces of late, idiomorphic quartz. Some parts of the altered metagranite, which macroscopically appear less altered since they are devoid of vugs, are actually completely resilicified by secondary quartz (samples B1 and B3 in Appendix A).

Altered amphibolite

Amphibolite is present in the strongly altered part of the metagranite. This rock is also severely altered but has no vugs. The altered amphibolite consists almost exclusively of stained plagioclase feldspar and opaque-looking aggregates intergrown with quartz (Figure 6-4a). Accessory, clear apatite grains appear unaffected by the alteration. The composition of the plagioclase feldspar has been altered to pure albite (see sample at level 290.03 m in Appendix B). The opaque-looking aggregates, which were probably hornblende prior to alteration, consist of chlorite with minute hematite and Ti-oxide grains (Figure 6-4b), similar to the dark aggregates in the altered metagranite. One small grain of titanite was identified; this is probably a remnant from the amphibolite-facies assemblage.

Figure 6-4. *Altered amphibolite (sample KFM02A, 290.03 m, B2 in Appendix A).*

a) Overview shows that the altered amphibolite consists of stained plagioclase feldspar and opaque-looking aggregates with interstitial quartz. Width of view is c 20 mm.

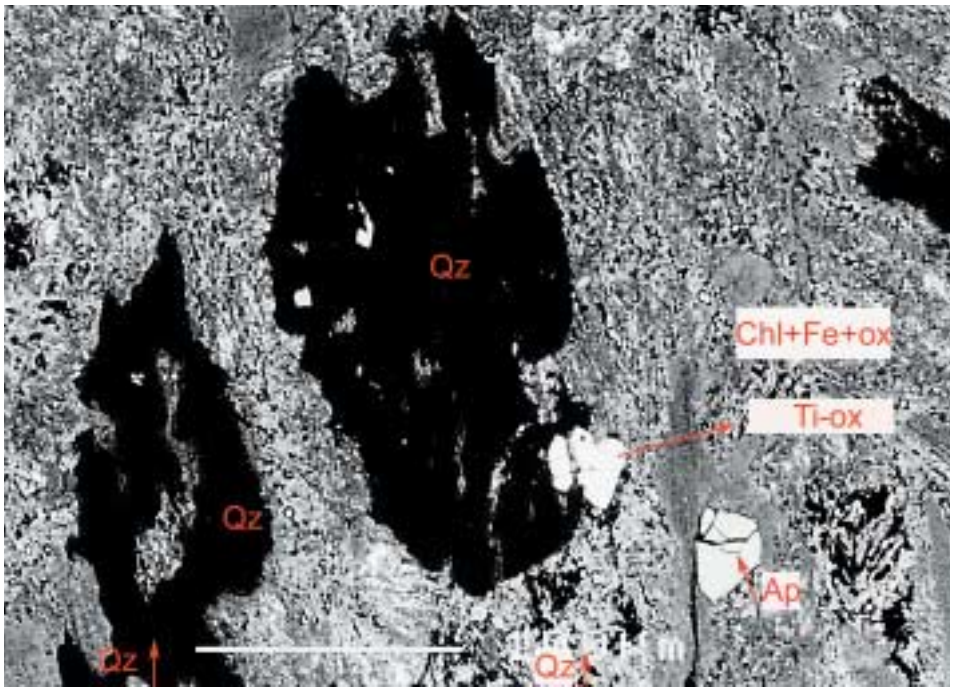

b) Detailed BSE image of an opaque-looking aggregate. The aggregate is composed of chlorite (light grey) that is heavily stained by tiny hematite grains (bright). It also contains interstitial quartz (black) and grains of Ti-oxide (bright). Scale bar = 0.1 mm.

6.1.2 EDX analyses and mineral compositions

Table 6-1 presents semi-quantitative EDX analyses of minerals from three different rocks, unaltered metagranite without vugs (A2 in Appendix A at 317.26 m), strongly altered metagranite with vugs (D2 at 295.82–295.89 m) and altered amphibolite (B2 at 290.03 m). A summary of these mineral compositions is provided below:

Plagioclase feldspar

Analysis of Na is problematic (see above) which is why the stoichiometric proportions of Si, Al and Ca (especially Al and Ca) in the analysis best determine the composition of the plagioclase feldspar. Plagioclase feldspar in unaltered metagranite has c 20 mole % anorthite component ($CaAl_2Si_2O_8$) and is classified as oligoclase. Plagioclase feldspar in altered metagranite with vugs, both "old" (stained) and newly precipitated grains, is pure albite ($NaAlSi_3O_8$). "Old" (stained) plagioclase feldspar in the altered amphibolite is also pure albite.

K-feldspar

K-feldspar is pure $KAlSi_3O_8$ in both unaltered and altered metagranite and in the amphibolite. Very small amounts of Ti (c 0.2 weight % TiO_2) were detected in K-feldspar in both metagranites, and small amounts of Na (0.3–0.6 weight % Na_2O) in the K-feldspar in the altered metagranite.

Epidote

Epidote occurs in the unaltered metagranite. It is to 85–90% a pure end-member epidote ($Ca_4Fe^{3+}{}_2Al_4Si_6O_{24}(OH)_2$) with 10–15% clinozoisite component ($Ca_4Al_6Si_6O_{24}(OH)_2$). The epidote contains small amounts of Mn (c 0.4 weight % MnO).

Biotite

The Fe/(Fe+Mg) ratio of biotite in unaltered metagranite is c 0.73. The biotite contains some Ti (c 2 weight % TiO_2) and subordinate amounts of Mn (c 0.5 weight % MnO).

Chlorite

During analysis of chlorite in both the altered metagranite and the amphibolite, care was taken to select surfaces without hematite staining (cf Figures 6-2d and 6-4b). However, it is possible that extremely fine hematite grains (beyond the resolution of the electron microscope) do occur in the analysed spots.

In the altered metagranite, two textural types of chlorite were analysed, from pseudomorphs after biotite (D2 chl1–3) and from radial aggregates in vugs (D2 chl4–6). Fe/Fe+Mg ratios are uniform in all the chlorites that have been analysed. Assuming that all Fe is ferrous in character, the values range between 0.53 and 0.57. Fe/Fe+Mg ratios of two chlorites in the altered amphibolite yielded values of 0.50 and 0.59.

Ti- and Fe-oxides

Ti-oxide (probably anatase) is almost pure, but commonly contains subordinate amounts of Fe. Fe-oxide grains in chlorite and feldspar are too small to analyse, generally smaller than 1 micrometer. XRD analyses (see below) demonstrate that the Fe-oxide mineral is hematite.

Zircon

Zircon spectra were collected but not analysed quantitatively. Spectra from unaltered zircon consist solely of Zr and Si. Spectra from altered zircon contain Ca, Al and some Fe in addition to Zr and Si. Three very small grains (one of them > 5 micrometers) with typical altered zircon spectra were found to also contain a clear Th peak.

Table 6-1. Energy-dispersive X-ray (EDX) analyses of minerals from unaltered metagranite without vugs (A2, 317.26 m), strongly altered metagranite with vugs (D2, 295.87–295.89 m) and altered amphibolite (B2, 290.03 m).

	A2 pl1	A2 pl2	A2 pl3	D2 oldpl1	D2 oldpl2	D2 newpl1	D2 newpl2	B2 pl1	B2 pl2	A2 Kfsp1	D2 Kfsp1	D2 Kfsp2	B2 Kfsp1
Wt-% oxide (all Fe calculated as FeO)													
SiO2	63.28	62.53	62.27	67.88	67.92	68.04	68.41	68.42	68.06	64.8	64.37	64.84	64.5
TiO2										0.26	0.25	0.16	
Al2O3	22.91	22.65	22.45	19.17	19.36	19.16	19.26	19.31	19.35	18.74	18.45	18.68	18.3
FeO	0.05	0.97	0.16		0.15	0.25	0.13					0.3	0.82
MnO													
MgO													
CaO	4.27	4.11	4.27					0.1	0.12				
Na2O	7.41	7.11	7.3	9.15	9.2	9.35	9.18	8.65	9.55		0.61	0.33	
K2O	0.21	0.21	0.21							17.07	16.71	16.81	17.44
Total	98.13	97.58	96.66	96.2	96.63	96.8	96.98	96.48	97.08	100.87	100.39	101.12	101.06
Stoichiometry (Fe as Fe2+)													
Si	2.83	2.84	2.84	3.05	3.04	3.04	3.05	3.06	3.04	2.98	2.99	2.98	2.99
Ti										0.01	0.01	0.01	
Al	1.21	1.21	1.21	1.02	1.02	1.01	1.01	1.02	1.02	1.02	1.01	1.01	1,00
Fe			0.01		0.01	0.01	0.01					0.01	0.03
Mn													
Mg													
Ca	0.21	0.2	0.21					0.01	0.01				
Na	0.64	0.63	0.65	0.8	0.8	0.81	0.79	0.75	0.83		0.05	0.03	
K	0.01	0.01	0.01							1,00	0.99	0.99	1.03
Total	4.9	4.89	4.93	4.87	4.87	4.87	4.86	4.84	4.9	5.01	5.05	5.03	5.05
based on O	8	8	8	8	8	8	8	8	8	8	8	8	8

Table 6-1. Continued.

	A2 epid1	A2 epid2	A2 biot1	A2 biot2	D2 chl1	D2 chl2	D2 chl3	D2 chl4	D2 chl5	D2 chl6	B2 chl1	B2 chl2	D2 Ti-ox
Wt-% oxide (all Fe calculated as FeO. except for epidote for which Fe has been recalculated as Fe2O3)													
SiO2	37.82	37.99	35.57	35.51	29.23	28.87	28.85	29.32	29.79	29.23	26.52	29.46	
TiO2			2.19	2.16							0.26		101.38
Al2O3	23.01	23.71	16.15	14.46	17.69	17.39	17.82	17.42	17.18	17.57	14.98	16.74	
FeO	15.12	14.62	27.18	27.1	25.26	25.48	26.04	25.92	25.21	25.17	28.12	22.79	2.2
MnO	0.45	0.44	0.54	0.56	0.51	0.47	0.46	0.61	0.58	0.53	0.24	0.32	
MgO			5.52	5.62	11.97	12.15	11.2	12.06	12.55	12.76	10.95	12.98	
CaO	24.58	24.51			0.58	0.57	0.58	0.62	0.51	0.52	0.46	0.5	
Na2O													
K2O			10.23	10.27	0.1	0.09	0.14	0.13	0.11	0.08	0.2	0.26	
Total	100.98	101.27	97.38	95.68	85.34	85.02	85.09	86.08	85.93	85.86	81.73	83.05	103.58
Stoichiometry (Fe as Fe2+. except for epidote where Fe has been recalculated as Fe3+)													
Si	5.91	5.9	5.56	5.53	6.31	6.27	6.28	6.29	6.37	6.26	6.15	6.46	
Ti			0.26	0.25							0.04		0.98
Al	4.23	4.34	2.97	3.02	4.5	4.45	4.57	4.41	4.33	4.44	4.1	4.33	
Fe	1.78	1.71	3.55	3.53	4.56	4.63	4.74	4.65	4.51	4.51	5.46	4.18	0.02
Mn	0.06	0.06	0.07	0.07	0.09	0.09	0.08	0.11	0.11	0.1	0.04	0.06	
Mg			1.29	1.31	3.85	3.93	3.63	3.86	4,00	4.07	3.79	4.24	
Ca	4.11	4.08			0.14	0.13	0.13	0.14	0.12	0.12	0.11	0.12	
Na													
K			2.04	2.04	0.03	0.02	0.04	0.04	0.03	0.02	0.06	0.07	
Total	16.09	16.09	15.74	15.75	19.48	19.52	19.47	19.5	19.47	19.52	19.75	19.46	1.00
based on O	25	25	22	22	28	28	28	28	28	28	28	28	2
Fe/Fe+Mg			0.73	0.73	0.54	0.54	0.57	0.55	0.53	0.53	0.59	0.50	

6.1.3 X-ray diffraction data and mineral compositions

Twelve samples have been selected for mineral identification by X-ray diffraction analysis from the alteration zone at the 250–300 m depth interval. Seven of these samples consist of scrapings from the walls of vugs in the dominant, medium-grained metagranite and one sample is from the scrapings of vugs in pegmatite. One sample was taken from an altered amphibolite at the level 290.03 m and another from a small segregation of pale-coloured material at the level 288.12–288.17 m. Two samples were also taken from a fine-grained coating in the non-cohesive section associated with amphibolite at 291.0–292.5 m and along a fracture that separates amphibolite and metagranite at the level 294.59 m. The X-ray diffractograms of all the analysed samples are shown in Appendix B. A brief summary of the results is provided below.

A characteristic feature of almost all the samples analysed is the presence of hematite, chlorite and plagioclase feldspar (albite). This mineral assemblage is present in the samples from the walls of the vugs, from the sample extracted from the non-cohesive zone at 291.0–291.5 m and from the fracture filling at 294.59 m. At the 262.20–262.21 m level, a mineral aggregate composed of pure hematite crystals was identified (see Appendix B). The altered amphibolite is also dominated by hematite, chlorite and albite, with subordinate quartz. It is possible that the chloritisation of primary mafic minerals released excess silica and accounts for the precipitation of quartz. Minor amounts of a mica-type mineral, here tentatively interpreted as an illite, is present in at least some of the vugs, in the amphibolite and in the fine-grained material from the non-coherent section at 291.0–291.5 m. The pale-coloured segregation at 288.12–288.17 m is composed of calcite.

The mineral composition of the vugs is well-illustrated by the sample from the 256.10–256.39 m level. Two fractions of this sample were analysed, the whole sample and the fine-grained fraction of the sample. During the analysis of the whole sample, the material was placed in the special sample holder, i.e. the analysis was performed with a random orientation of mineral grains. Only the peaks from the major minerals in the sample, hematite and plagioclase feldspar (albite), are prominent in this diffractogram (Figure 6-5).

The fine-grained fraction of the sample was analysed with a preferred orientation of the mineral grains (oriented sample). This is the routine adopted for qualitative analyses of clay minerals. Using this technique, 00l-peaks of phyllosilicates, which represent the C-planes in the mineral lattice, are prominent. The diffractogram obtained from the analysis of the fine-grained fraction displays a strong peak from hematite (Figure 6-6). Peaks from chlorite, biotite, plagioclase feldspar (albite) and possibly anatase and rutile are also present (Figure 6-6).

Chlorite, which is present in all samples except those composed solely of hematite and calcite, differs from the chlorites found in the /PDF, 1994/ database. As illustrated by the positions of peaks at lower 2-theta angles in the X-ray diffractograms (see Appendix B), the d-values of 001-peaks obtained are somewhat larger than the d-values for the chlorite which shows the best fit in the /PDF, 1994/ database (chlorite number 16-0362). Intensity ratios between peaks also differ, e.g. between the 001- and 002-peaks at 6.2° and 12.4° (2-theta), respectively. In part, this may be explained by the fact that the pattern for chlorite in the /PDF, 1994/ database represents analyses with a random orientation of mineral grains, while most chlorite crystals in the present work are more or less oriented. This results in stronger peaks at the low 2-theta angles.

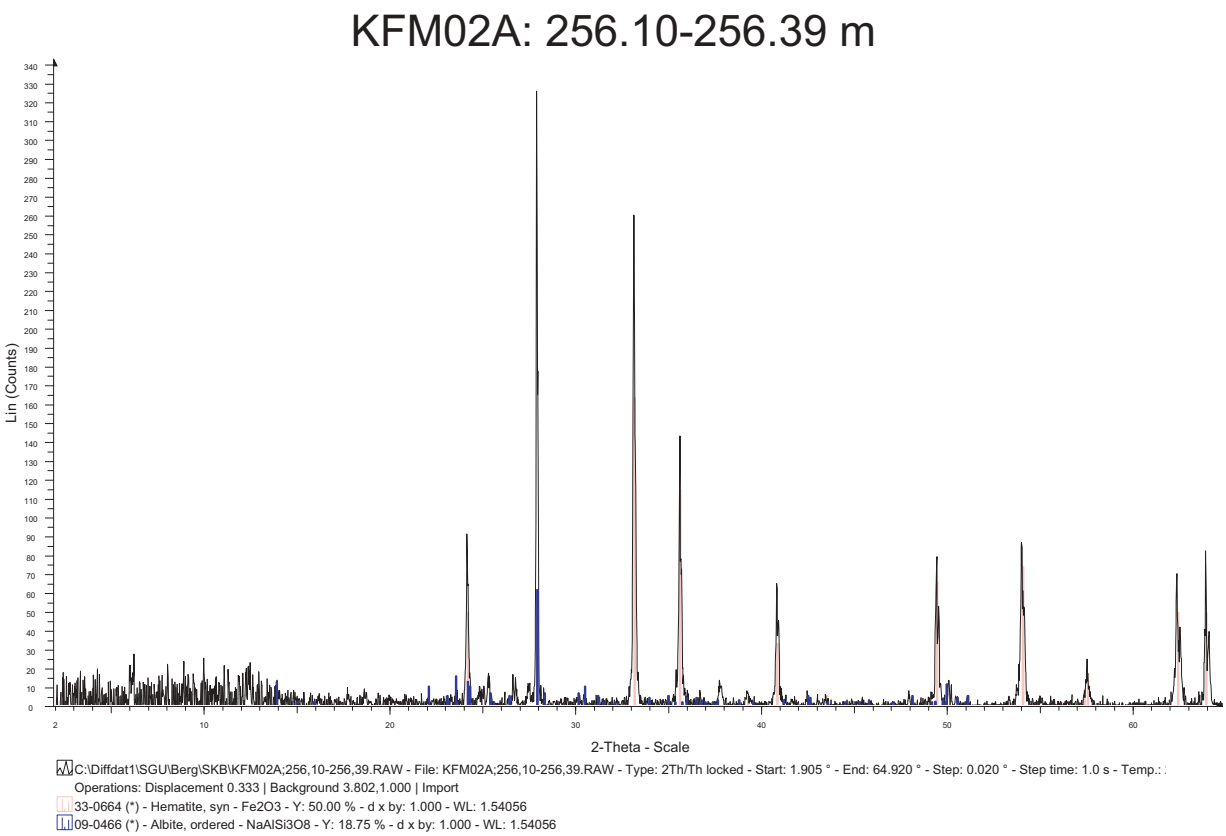

Figure 6-5. *X-ray diffractogram of the whole sample from the 256.10–256.39 m depth interval.*

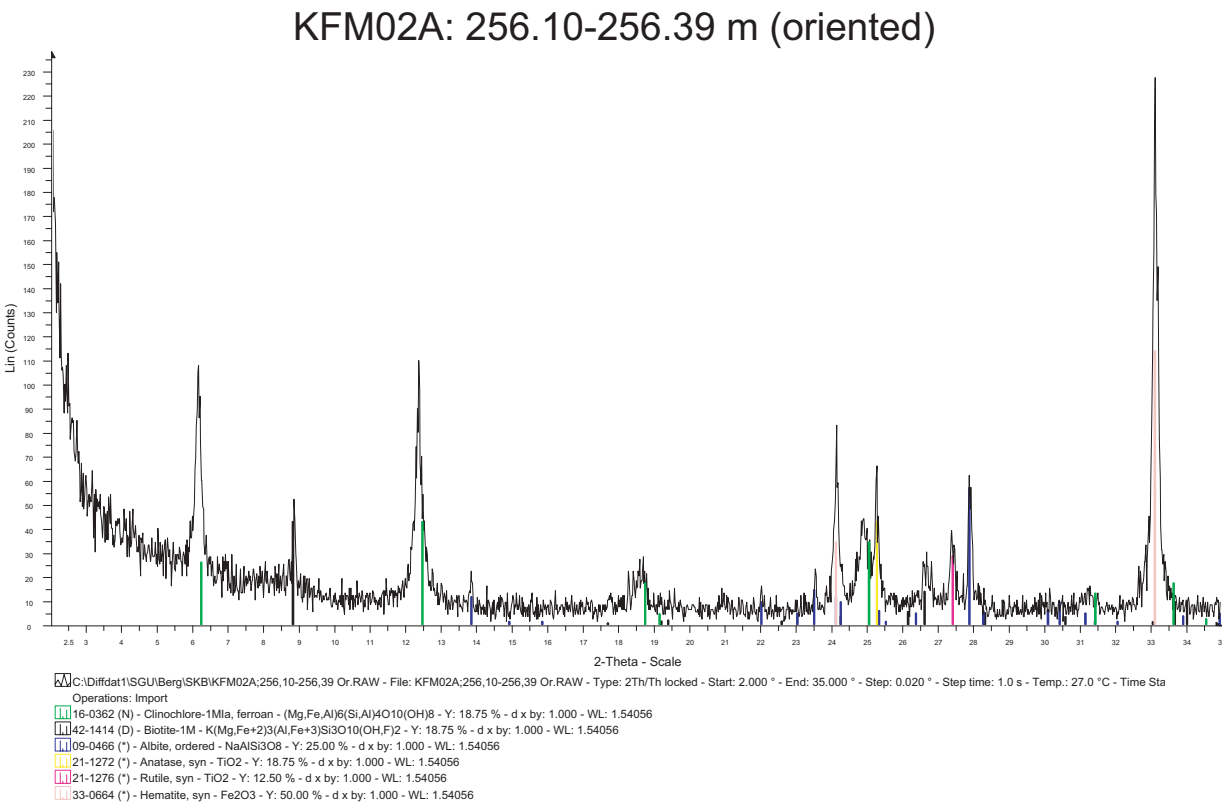

Figure 6-6. *X-ray diffractogram of the fine-grained fraction of the sample from the level 256.10–256.39 m depth interval.*

For identification purposes, most samples were saturated with ethylene glycol (EG) to investigate whether swelling layers, e.g. smectite or vermiculite, are present in the chlorite. In one of the samples (256.10–256.39 m depth interval), saturation with glycerol was also carried out. Saturation of the samples was followed by heating to 450°C. If swelling layers are interstratified with chlorite, the chlorite 001-peak should change in position to a lower 2-theta angle when saturated with these organic molecules. Heating causes the collapse of swelling layers and a change in the position of the 001-peak to a higher 2-theta angle. Since no changes of the X-ray diffraction pattern could be detected in the analysis of an oriented sample after saturation with organic material and heating (see, for example, the sample from the 275.20 m level in Appendix B), it is apparent that the chlorite is not interstratified with swelling layers.

Chlorite is a complex group of minerals with similar structure. It is tentatively suggested that different types of chlorite with somewhat different crystal structures are present even within the same sample. For example, in the sample from the 291.17 m level, the 001-peak at 6.2° (2-theta) is very strong, stronger than the 002-peak at 12.5° (2-theta). The peaks at higher order are broad, e.g. the 004-peak at 25° (2-theta) displays, in fact, three separate maxima when magnified (Figure 6-7), at 3.573 Å, 3.560 Å and 3.546 Å. The 002-peak also shows some tendency to be an integration of several peaks. However, at the low angle of 6.2° (2-theta), the 001-peaks are not resolved in the diagram, but interfere into one peak with a maximum at 14.4 Å. It is possible that an interference between diffferent chlorites may, at least partly, explain the relatively strong intensity of the 001-peak.

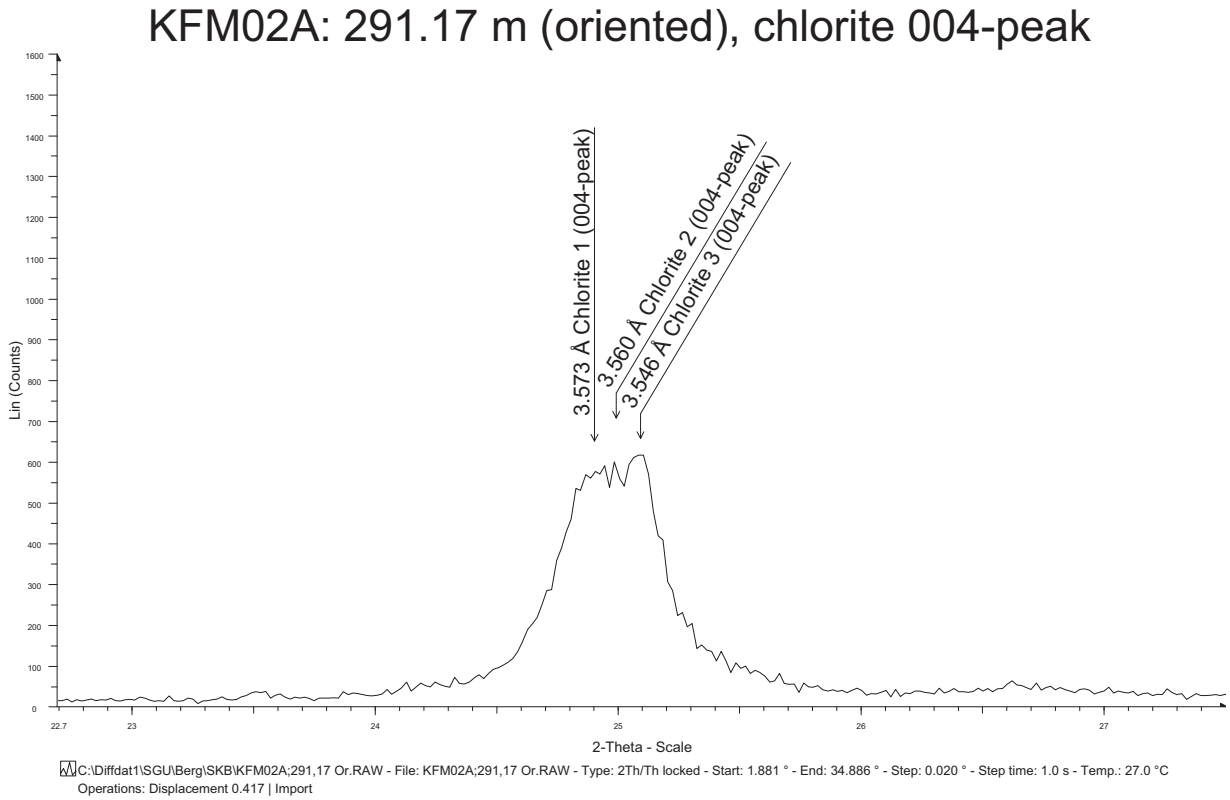

Figure 6-7. *Part of the X-ray diffractogram of the sample from the 291.17 m level with a magnified chlorite 004-peak.*

6.2 Literature review of episyenites

6.2.1 What is episyenite?

The mineralogical investigations show that the alteration process which has affected the metagranite in KFM02A has involved a loss of quartz with the formation of vugs and is associated with, amongst other features, the replacement of oligoclase by albite. The term episyenite /Le Maitre, 2002 and references therein/ was coined by uranium exploration geologists for an igneous-looking rock of syenitic composition that:

1. displays vugs produced by hydrothermal dissolution of quartz crystals,
2. is commonly associated with alkali metasomatism (Na or K),
3. can ultimately host uranium ore deposits.

In older literature, these rocks have been termed pseudosyenite. It is apparent that the process that can be referred to as episyenitisation has affected the metagranite in KFM02A.

In episyenites, the grain size and texture of the protolith are preserved, but quartz has been removed and replaced by vugs. Episyenite commonly forms small bodies, less than 100 m across, which are pipe-like, irregular sheets or are ovoid in shape. These bodies occur within the granitic protolith /e.g. Recio et al, 1997; Petersson 2002; and references therein/. Episyenites are either deep red or white in colour and have sharp contacts (maximum 2–3 cm thick) to the granitic protolith. If more than one granitic rock type is present, episyenite bodies commonly traverse all the different rock types. Older studies describe occurrences in Ireland /Walker and Leedal, 1954/ and France /Cathelineau, 1986 and references therein/. At the present day, examples of episyenite are known from different parts of the world. A compilation is provided in /Petersson, 2002/.

The relationship between episyenite bodies and deformational structures is discussed in many publications. Many episyenites, notably episyenites with secondary mineralisations, can be spatially correlated with faults or fracture zones /e.g. Recio et al, 1997 and references therein/. However, some episyenites bear no distinctive relationship to faults or fracture zones, and some are virtually unfractured. /Petersson, 2002/ noted that the vast majority of these occurrences are barren with respect to mineralisation, and speculated that faults associated with episyenites have facilitated late access to metal-bearing fluids rather than the initial episyenitisation.

6.2.2 Common alterations, vug fillings and ore mineralisation in episyenites

The dissolution of quartz and vug formation are often associated with other mineralogical changes. /Cathelineau, 1986/ described four basic types:

1. Quartz dissolution.
2. Quartz dissolution accompanied by albite crystallisation, so-called albitisation.
3. Quartz dissolution accompanied by K-feldspar crystallisation.
4. Late alteration (muscovite or clay minerals).

In addition, dark minerals are often altered to chlorite, hematite and anatase.

Vug fillings are common but vary in composition and complexity. Common minerals are quartz, albite, adularia, carbonates, muscovite, chlorite, apatite, hematite, anatase and pyrite /Cathelineau, 1986; Recio et al, 1997; Petersson and Fallick, 2002; and references therein/. Episyenites are also known as hosts for secondary, epigenetic ore mineralisations, notably U, Sn-W-Mo, Au and Pb-Zn-Cu.

6.2.3 Episyenitisation – the process

There is general agreement that hydrothermal solutions are responsible for the dissolution of quartz and associated albitisation or K-feldspar crystallisation and that, in many episyenites, fluid interaction and mineral precipitation have occurred in more than one stage. Thus, many episyenites are complex rocks, and suggestions differ as to whether the fluids responsible for the quartz dissolution and alkali metasomatism were derived from magmatic, meteoric or other sources.

Stable isotopes and fluid inclusion data on secondary mineral phases suggest that, in many episyenites, meteoric fluids have been invoked during the vug-filling stages. Most information concerning the fluids responsible for quartz dissolution has, by necessity, been obtained indirectly from the minerals *assumed to be* coeval with the dissolution. There is an inherent difficulty in such interpretations since episyenites have commonly experienced a multistage evolution, with dissolution, precipitation during one or more stages and, commonly, late alteration. In addition, both fluid inclusions and oxygen isotopes in feldspars are susceptible to changes or reactivation at low temperatures /e.g. discussion in Petersson and Fallick, 2002/.

The so-called retrograde dissolution model /e. g. Cathelineau, 1986/ suggests that episyenitisation was caused by meteoric fluids with low to moderate salinity, at low pressures (0.3–1.8 kbar, op. cit; 0–0.9 kbar according to /Petersson and Fallick, 2002/) and at temperatures corresponding to greenschist facies (250–400°C). At decreasing temperatures in the vicinity of c 360–400°C, the solubility of quartz in aqueous fluids undergoes a dramatic increase which permits originally quartz-saturated fluids with appropriate chemistry to become undersaturated and dissolve quartz from the rock. When the temperature decreases below 360°C, the solubility of quartz decreases again and quartz can then precipitate from the fluids.

Other models propose that quartz dissolution and associated albitisation/microclinisation were caused by the action of late-magmatic, so-called deuteric fluids /e.g. Dempsey et al, 1990; Recio et al, 1997; Petersson 2002; and references therein/. These interpretations rely mainly on oxygen isotope data from feldspars that are considered to be coeval with the episyenite formation and that show magmatic or mixed magmatic and meteoric values. The Bohus granite in southwestern Sweden is an example where stable isotope data of late-stage quartz indicate high-temperature crystallisation. /Petersson et al, 2002/ and /Petersson and Fallick, 2002/ suggest late-magmatic alteration by a deuteric, hypersaline fluid generated *in situ* during the final crystallisation of the interstitial melt, a scenario which, in the case of the Bohus granite, implies conditions of c 670°C and 4 kbar. The same authors remark that the field geometry of many episyenites, i. e. clusters of separate, sharply defined bodies rather than localisation along faults or fracture zones, is more consistent with the *in situ* model rather than with the classical retrograde dissolution model. The latter requires high fluid/rock ratios and, by inference, permeable and efficient channelways for fluids such as faults or fracture zones.

6.2.4 Episyenite occurrences in Sweden

Two areas with occurrences of episyenite in Sweden have been described in scientific publications. These include the Arjeplog-Arvidsjaur-Sorsele province in northern Sweden and the Bohus granite on the southwest coast.

In the Arjeplog-Arvidsjaur-Sorsele province, episyenites are associated with thirty known uranium mineralisations /Hålenius and Smellie, 1983; Smellie and Laurikko, 1984; Hålenius et al, 1986/. Episyenitisation has affected uranium-enriched granites and rhyolitic porphyries that are c 1,890–1,840 million years old and involved the introduction of Na, Ca and base metal sulphides. Uraninite is confined to the episyenitised zones and occurs as impregnations and fillings along microfractures. The precipitation of uraninite is interpreted to have followed the episyenitisation process and has been dated by the U-Pb method at c 1,750 million years /Hålenius et al, 1986/. It is suggested that hydrothermal fluids moved along pre-existing fault zones and more permeable lithological horizons and that these fluids gave rise to alteration and eventually uranium mineralisation. Intrusion of granites was coeval with regional metamorphism in the province and probably provided the necessary temperature gradient to drive the hydrothermal fluid movement /Hålenius et al, 1986/.

The character of episyenites in the Bohus granite on the southwest coast has recently been documented regarding field relations, petrography, geochemistry, geochronology, fluid inclusions and stable isotopes /Petersson, 2002/. The alteration process is considered to have taken place in successive stages:

1. Initial dissolution of quartz accompanied by albitisation of plagioclase.
2. Subsequent infilling in the vugs by apatite, micas, hematite, anatase and quartz (J Petersson, personal communication, 2003).
3. Sporadic argillitic alteration and precipitation of ankerite /Petersson and Eliasson, 1997; Petersson et al, 2002/.

Xenotime occurs in the micaceous vug-filling assemblage in one of the episyenites. U-Pb dating of this xenotime has given an age of 252 ± 8 Ma (Late Permian), suggesting that this vug-filling event took place simultaneous with the development of the nearby Oslo Rift /Petersson et al, 2001/, c 670 million years after formation of the granite. Fluid inclusions and stable isotopes have equilibrated or re-equilibrated during the late events. However, at a few localities, oxygen isotopes of quartz, which is interpreted to have formed after albitisation, yield magmatic values. These data indicate that fluids which caused the alteration are deuteric in character /Petersson et al, 2002/.

An additional occurrence of desilicified granite has been reported from Stripa, in central Sweden. In a drillcore at Stripa, reddened, porous, quartz-deficient granite was encountered in two zones, 1.7 and 3.0 m wide /Carlsten, 1985/, at the 360 m level in the Stripa mine. This quartz-deficient granite has not been documented in detail. /Eliasson, 1993/ described grey, leached granite along the 81 to 85 m core length in drillhole D5, at the 382–390 m mine level.

The episyenitisation at Forsmark (this study) is associated with reddening of the rock, similar to reddening reported from other localites (examples in Sweden include Stripa and parts of the Bohus granite). In other places, episyenitisation is associated with whitening of the rock (e.g. some of the occurrences in the Bohus granite). /Eliasson, 1993/ investigated the petrography, geochemistry and petrophysics of red-coloured granite, which occurs adjacent to fractures, at Äspö and Stripa. At Stripa, the red colour is caused by hematite and Fe-oxyhydroxide along microfractures, grain boundaries and, subordinately,

in the main minerals. The oxidation and precipitation of iron is interpreted to be related to retrograde alteration of chlorite to muscovite. The granite at Äspö is strongly red-coloured along fractures that are filled with epidote, prehnite, calcite and chlorite. The strong reddening of the granite is caused by very fine-grained dispersed Fe-oxyhydroxides/hydroxides that are interpreted to have formed during a final low temperature stage at c 150–250°C. The mineralogical features of the altered Äspö granite, which include replacement of biotite by chlorite, of plagioclase feldspar by albite and sassurite, and of magnetite by hematite, show clear similarities with episyenites. However, there has not been any loss of quartz in the rock. The altered plagioclase feldspar contains numerous small micropores that are interpreted as dissolution voids.

7 Conclusions

The following conclusions are made concerning vug formation, alteration and new grain growth in drillcore KFM02A:

- Strongly altered and porous rocks occur in three zones. Two of these zones are narrow and occur at 175 and 180 m depth. One is considerably broader, traverses different rock types and occurs within the 250 and 300 m depth interval.
- The alteration involved loss of quartz in metagranitic rocks and gave rise to rocks composed predominantly of feldspars and vugs. Ca-bearing plagioclase was replaced by pure albite in both altered metagranite and amphibolite. Fe-Mg minerals were replaced by chlorite, hematite and Ti-oxide. K-feldspar grains were resorbed along the vug walls.
- The vug formation is associated with strong reddening of the rock that apparently was caused by staining of plagioclase feldspar by minute hematite grains.
- Precipitated minerals on the vug walls are albite, quartz, chlorite, hematite and Ti-oxide. Some parts of the altered zones remain devoid of quartz but, in most cases, new quartz has precipitated in the vugs. Quartz is commonly the latest mineral and has an idiomorphic habit. Some parts of the altered metagranite are completely resilicified with quartz filling the former vugs.
- The chlorite is not interstratified with swelling layers, e.g. smectite or vermiculite.
- The alteration mineralogy indicates that significant exchange of elements has taken place, notably loss of Si and Ca and gain of Na. This alteration was caused by the action of hydrothermal fluids.
- The mimicking of the ductile fabric by the vugs, the preservation of open vugs, and the strain-free character of newly precipitated albite and quartz demonstrate that the alteration, the vug formation and the vug filling are all younger than, and genetically unrelated to, the intrusion of the granite and the subsequent ductile deformation and metamorphism.
- The vug formation, mineral alteration and mineral precipitation are typical for Type II episyenitisation as described by /Cathelineau, 1986/. This phenomenon is a well-established feature in several granites throughout the world.
- The character of new minerals along the walls of the vugs, within the non-cohesive section in the lower part of the 250–300 m depth interval and within a fracture filling are identical. This suggests that the process (or processes) responsible for new mineral growth in these different structural domains is (are) similar.
- It is suggested that the hydrothermal alteration and vug formation occurred under relatively low pressures and at temperatures corresponding to the greenschist facies. It is envisaged that fluids percolated through discrete channelways in the metagranite and that this event took place distinctly later than the ductile deformation and amphibolite-facies metamorphism. It is speculated that brittle deformation and injection of hydrothermal fluids may have been connected with the regional tectonic events that guided the intrusion of younger igneous rocks at high crustal levels during the latest part of the Palaeoproterozoic or during the Mesoproterozoic.

- No metal-bearing mineralisations of potential economic interest have been found in the vuggy and altered rocks. It is suggested that the absence of metallic mineralisation of economic interest is related to the geochemical character of the igneous rocks in the Forsmark area and its immediate surroundings. These rocks formed in an active continental margin setting and contain low contents of, for example, U, Sn, Mo and W, elements that are known to form mineralisations in association with episyenites in other parts of the world.

8 Suggestions for further studies

The present study forms a basis for further investigations of the vuggy metagranite and associated rocks. As a starting point, the literature review presented in this report made use of the recently published thesis by /Petersson, 2002/ and the papers presented therein /Petersson and Eliasson, 1997; Petersson et al, 2001, 2002; Petersson and Fallick, 2002/. Extensive reference lists that do not need to be repeated here are provided in these papers. It is recommended that these references are consulted in more detail in connection with especially petrogenetic investigations such as whole-rock geochemistry, stable isotope work, fluid inclusion microthermometry and geochronology. The suggestions for further studies are summarized below.

Geometry and relationship to brittle structures

The three-dimensional geometry of the zones and bodies of vuggy metagranite at Forsmark is of key importance and cannot be determined from the data from this drillcore alone. Data from additional boreholes is a prerequisite for this reconstruction. The episyenitisation has affected different rock types and is clearly bound neither by the lithological boundaries nor by the ductile structures.

In drillcore KFM02A, the most altered and vuggy rocks are very weak, fractured and locally have lost their coherence. Furthermore, the similarity of the mineral fillings in the vugs and along minor fractures in the lower part of the 250–300 m depth interval suggest that similar hydrothermal fluids were active in both these domains. Nevertheless, it was not possible to demonstrate during inspection of this single drillcore an unambiguous connection between the occurrence of vuggy and altered rocks and a more significant brittle structure (fracture or fault zone). Further drilling is necessary to confirm or refute a possible link between the vuggy and altered rocks and a more significant brittle structure.

Petrophysics

It is suggested that investigation of the petrophysical properties of the vuggy metagranite is included in future investigations. Five samples of medium-grained metagranite, in different states of episyenitisation, have been taken for this purpose (close to the sites for samples A2, A4, B3, C1 and D1/D2 described in Appendix A).

Whole-rock geochemistry

The interaction of elements between the host rock and the fluid during the episyenitisation alteration process can be evaluated by comparison of the whole-rock compositions of unaltered and altered metagranite. Five samples of medium-grained metagranite, in different states of episyenitisation, have been taken for this purpose (close to the sites for samples A2, A4, B3, C1 and D1/D2 described in Appendix A). /Baumgartner and Olsen, 1995/ present a graphical solution that can be applied for simple mass-balance analysis that is an improvement of the isocon method presented by /Grant, 1986/. An example of the application of this method is provided in /Petersson and Eliasson, 1997/.

Stable isotope and fluid inclusion studies

Stable isotope systematics of minerals precipitated in the vugs can be used to determine some aspects regarding the source of the hydrothermal fluids (e.g. magmatic and meteoric components). Fluid inclusion microthermometry can yield information on the composition and salinity of the trapped fluid. Both methods require careful and detailed investigations, as they might record conditions prevalent during cooling or reactivation, i. e. conditions later than and genetically unrelated to the precipitation of the host mineral.

Geochronological studies

Determination of the absolute age of episyenitisation requires a mineral that has precipitated during episyenitisation and is suitable for radiometric dating methods. The precipitated minerals identified in the present study (albite, quartz, chlorite, hematite and Ti-oxide) are not suitable for radiometric dating. Furthermore, there is the added difficulty to relate the timing of new mineral growth to the timing of alteration, including the formation of the vugs. However, it is possible that suitable, small-sized minerals occur locally in the episyenitised zones. Identification requires a careful search in additional samples by the aid of electron microscope and EDX equipment.

8 References

Baumgartner L P, Olsen S N, 1995. A least-squares approach to mass transport calculations using the isocon method. Economic Geologist 90, 1261–1270.

Carlsten S, 1985. Hydrogeological and Hydrogeochemical Investigations in Boreholes – Compilation of geological data. Stripa project. SKB internal report 85-04, 1–61.

Cathelineau M, 1986. The hydrothermal alkali metasomatism effects on granitic rocks; quartz dissolution and related subsolidus changes. Journal of Petrology 27:4, 945–965.

Dempsey C S, Meighan I G, Fallick A E, 1990. Desilication of Caledonian Granites in the Barnesmore complex, Co. Donegal: the origin and significance of metasomatic syenite bodies. Geological Journal 25, 371–380.

Drever S I, 1973. The preparation of oriented clay mineral specimens for X-ray diffraction analysis by a filter-membrane peel technique. American Mineralogist 58, 553–554.

Eliasson T, 1993. Mineralogy, geochemistry and petrophysics of red coloured granite adjacent to fractures. SKB technical report 93-06, 1–68.

Grant J A, 1986. The isocon diagram – A simple solution to Gresens' equation for metasomatic alteration. Economic Geologist 81, 1976–1982.

Hålenius U, Smellie J A T, 1983. Mineralizations of the Arjeplog-Arvidsjaur-Sorsele uranium province: mineralogical studies of selected uranium occurrences. Neues Jahrbuch fur Mineralogie Abhandlungen 147, 229–252.

Hålenius U, Smellie J A T, Wilson M R, 1986. Uranium genesis within the Arjeplog-Arvidsjaur-Sorsele uranium province, northern Sweden. In: Fuchs H D (Ed), Vein Type Uranium Deposits. TEC-DOC-361, IAEA, Vienna, 21–42.

Koistinen T, Stephens M B, Bogatchev V, Nordgulen Ø, Wennerström M, Korhonen J, 2001. Geological map of the Fennoscandian Shield, scale 1:2 000 000. Geological Surveys of Finland, Norway and Sweden and the North-West Department of Natural Resources of Russia.

Le Maitre R W (ed), 2002. Igneous rocks: A classification and glossary of terms. Recommendations of the International Union of Geological Sciences Subcommission on the Systematics of Igneous Rocks. Cambridge University Press, 240 pp.

PDF, 1994. Powder diffraction file computer data base. Set 1–43. International Centre for Diffraction Data, Park Lane, Swartmore, PA, USA.

Petersson J, Eliasson T, 1997. Mineral evolution and element mobility during episyenitization (dequartzification) and albitization in the postkinematic Bohus Granite, southwest Sweden. Lithos 42 (1–2), 123–146.

Petersson J, Whitehouse M J, Eliasson T, 2001. Ion microprobe U-Pb dating of hydrothermal xenotime from an episyenite; evidence for rift-related reactivation. Chemical Geology 175 (3–4), 703–712.

Petersson J, 2002. The genesis and subsequent evolution of episyenites in the Bohus granite, Sweden. Earth Sciences Centre Doctoral Thesis A75, Göteborg University.

Petersson J, Fallick A E, 2002. Episyenites: a critical evaluation of their proposed formation mechanisms. In: Petersson J, The genesis and subsequent evolution of episyenites in the Bohus granite, Sweden. Earth Sciences Centre Doctoral Thesis A75, Göteborg University, 11 pp.

Petersson J, Fallick A E, Broman C, Eliasson T, Sundvoll B, 2002. Imprints of multiple fluid regimes on episyenites in the Bohus granite, Sweden. In: Petersson J, The genesis and subsequent evolution of episyenites in the Bohus granite, Sweden. Earth Sciences Centre Doctoral Thesis A75, Göteborg University, 21 pp.

Recio C, Fallick A E, Ugidos J M, Stephens W E, 1997. Characterisation of multiple fluid-granite interaction processes in the episyenites of Avila-Bejar, central Iberian Massif, Spain. Chemical Geology 143 (3–4), 127–144.

SKB, 2002. Forsmark – site descriptive model version 0. SKB R-02-32, Svensk Kärnbränslehantering AB, 170 pp.

Smellie J A T, Laurikko J, 1984. Skuppesavon, northern Sweden: a uranium mineralisation associated with alkali metasomatism. Mineralium Deposita 19, 183–192.

Stephens M B, Bergman T, Andersson J, Hermansson T, Wahlgren C-H, Albrecht L, Mikko H, 2003. Forsmark. Bedrock mapping, stage 1 (2002) – outcrop data including fracture data. SKB P-03-09, Svensk Kärnbränslehantering AB.

Walker G P L, Leedal G P, 1954. The Barnesmore granite complex, county Donegal. The Scientific Proceedings of the Royal Dublin Society Series A 26:13, 207–243.

Appendix A

Descriptions of thin-sections

The minerals, textures and microstructures in the samples from drillcore KFM02A, that are observable with the help of a polarized light microscope, are described in Appendix A. Most samples from which the thin-sections were made are from the lower and broadest alteration zone at the 250–300 m depth interval. One sample was taken from the uppermost zone at 175 m depth (C3 below). The majority of samples consist of a medium-grained metagranite that displays various stages of alteration. This rock-type dominates the whole drillcore. The samples also include one altered amphibolite (B2 below) and two samples of a fine-grained metagranitoid that is somewhat poorer in dark minerals (C2 and C3 below) than the medium-grained metagranite.

The short descriptions of the samples, that were completed during sampling of the drillcore, have been translated to English and are provided in *italics*, in the text which follows below. During sampling of the drillcore, the character of alteration was judged optically as unaltered or slightly altered (sorted under A, below), altered without or with only a few vugs (B), altered with vugs (C) and strongly altered with vugs (D). Thin-sections reveal that the metagranites in category B are completely resilicified rocks that once had vugs.

A) Unaltered or slightly altered rocks

A1: Sample level 245.63. *Unaltered, fresh, (grey) red, medium-grained metagranite. The sample is taken 10 cm away from the contacts to a younger fine-grained granitoid and pegmatite.*

The metagranite is considerably finer-grained than its macroscopic medium-grained appearance. The rock is dominated by quartz and feldspars and contains minor amounts of dark minerals, mainly biotite or altered biotite. Quartz domains are elongate, but polycrystalline with very variable grain-sizes and shapes. Within the quartz domains, grain-boundaries are sutured, and individual grains show undulose extinction and deformation lamellae. These features suggest strain accommodation down to relatively low temperatures. Plagioclase feldspar grains are up to 2 mm large and stained. K-feldspar, up to 4 mm-sized grains, contains lamellae (exsolved albite or incipient albite replacement) that are often weakly lens- and S-shaped. Biotite is commonly altered to chlorite, in places with spindle-shaped pumpellyite lamellae. Epidote occurs frequently in association with biotite, often as fine grains along the rims of biotite but also as single larger grains (0.3 mm). It is variable in grain-size and shape. Accessory minerals are zircon (with oscillatory zonation), apatite, opaques and allanite. Red and opaque very fine-grained minerals (probably hematite) are found along microfractures and grain-boundaries, particularly in the quartz-rich domains. Single, very thin, late fractures are filled with an highly birefringent mineral.

A2: Sample level 317.26. *Unaltered, fresh, reddish grey, medium-grained metagranite.*

This section of the metagranite shows a high-temperature, foliated fabric that is defined by elongate quartz domains, 2–5 mm thick, alternating with feldspar-dominated domains, up to cm-thick, and aligned, thin streaks of dark minerals, mainly biotite (or its alteration products) and single opaque grains. The rock shows the same mineralogical, textural and microstructural features as A1 (above), but biotite and plagioclase feldspar show less chloritisation and sericitisation, respectively, and there is less hematite staining along microfractures etc. Myrmekite occurs locally.

A3: Sample level 245.60–245.63. *Non-porous (unaltered), (grey) red, medium-grained metagranitoid.*

This sample has been taken from the same depth as A1 (above) but the thin-section has been cut perpendicular to the planar and parallel to the linear, ductile deformational fabric. The sample is similar to A1 but the section shows a clear elongation of individual grains (biotite and large plagioclase feldspar grains) and mineral aggregates (notably quartz and plagioclase). The thin-section shows some relatively large and well-preserved plagioclase grains, the two largest of which are c 5 mm long and have tabular shapes.

A4: Sample level 351.57–351.59. *Reddish grey, non-porous, unaltered, medium-grained metagranitoid with a ductile linear fabric.*

The thin-section has been cut parallel to the linear, ductile deformational fabric. The sample shows the same mineralogical, textural and microstructural features as A2.

B) Altered rocks without or with few vugs

B1: Sample level 272.42. *Altered but non-porous, red, medium-grained metagranite.*

The metagranite is heavily stained by opaques and large parts of the section are aggregates of fine-grained minerals, mostly feldspars and opaques. Very fine-grained minerals stain the plagioclase feldspar. In contrast to the unaltered metagranites (A1–A4 above), the quartz is clearly secondary, strain-free, has straight grain-boundaries and fills volumes that have previously been voids. Abundant small inclusions (probably both solid and fluid) occur in the quartz. Biotite is no longer present but has been replaced by opaque-looking minerals, or is nearly opaque with a weak brownish or greenish tint. These mineral aggregates are commonly fibrous in character. Single muscovite grains occur in association with the replacements after biotite.

B2: Sample level 290.03. *Fine-grained amphibolite, somewhat altered but non-porous. Surrounded by strongly altered and porous, medium-grained metagranite.*

The rock consists of heavily stained plagioclase feldspar grains (> 50%) that are 1–1.5 mm in grain-size. This staining gives the plagioclase feldspar a reddish beige colour in hand-specimen. The remaining rock is composed of opaque-looking minerals or is nearly opaque with a brownish or greenish tint where grains are very thin. These aggregates are commonly fibrous in character and intergrown with quartz. Small rounded clear grains of apatite occur in plagioclase feldspar and in the dark domains. Neither hornblende nor biotite is present in the altered amphibolite.

B3: Sample level 263.51–263.54. *Altered, somewhat porous, red, medium-grained metagranitoid.*

The thin-section has been cut perpendicular to the planar and parallel to the linear, ductile deformational fabric. The section shows a clearly elongate ductile fabric. It is defined by thin planar aggregates of opaque-looking pseudomorphs after biotite, and the elongate shape of aggregates of quartz and feldspar, respectively. Mineralogically, texturally and microstructurally, the sample is identical to the altered, medium-grained metagranite with vugs (C and D, below), but the rock has only a limited number of small open vugs. The former vugs are filled with secondary, strain-free quartz with straight grain-boundaries.

C) Altered rocks with vugs

C1: Sample level 278.19. *Relatively strongly altered, porous and strongly red, medium-grained metagranite.*

The metagranite is composed of plagioclase feldspar, K-feldspar and quartz. Plagioclase is stained by very fine-grained minerals, as are plagioclase lamellae in K-feldspar. Dark mineral aggregates are opaque (or nearly opaque) and many of them are fibrous in shape. Small, single muscovite grains are present in association with the opaque minerals. Optically identifiable chlorite occurs in subordinate amounts. Accessory minerals are apatite and zircon.

Open vugs in the metagranite are irregular in shape, 1–6 mm long, rimmed or partly filled by secondary quartz, feldspar and, locally, opaques. Grain-sizes of secondary feldspar and quartz are variable. Very fine-grained thin rims of colourless minerals occur as well as larger (up to 3 mm) quartz grains that fill former cavities. Crystal faces of secondary feldspar and, especially, quartz are generally sharp.

C2: Sample level 289.61. *Relatively strongly altered, porous and strongly red, fine-grained metagranitoid.*

This metagranite is rich in vugs, commonly 2–6 mm long, but poor in both quartz and dark minerals. One 4 mm large K-feldspar megacryst, with abundant plagioclase feldspar exsolutions in the core, occurs in the thin-section; feldspar grains are otherwise finer-grained (commonly 0.5–2 mm). Plagioclase feldspar is stained and the small amounts of dark minerals consist of scattered, often fibrous, opaque-looking minerals and dull greenish chlorite. The feldspars fringing the vugs show, in places, sharp crystal faces; elsewhere, these minerals show embayments. In many vugs, a thin rim composed of secondary, very fine-grained, colourless minerals occurs on the feldspars. This rim is marked by minute brownish inclusions. Secondary quartz is present, but in very subordinate amounts.

C3: Sample level 174.33–174.36. *Relatively strongly altered, porous, red, fine-grained metagranitoid.*

This sample was taken from the uppermost alteration zone. The thin-section has been cut perpendicular to the planar and parallel to the linear, ductile deformational fabric. The thin-section shows a strongly elongate ductile fabric defined by feldspar domains, sparse yet large K-feldspar crystals, and sparse amounts of dark minerals. The rock is almost quartz-free, but vugs after quartz are abundant, with an elongate shape and up to 1 cm long. Two tabular K-feldspar megacrysts, 5 and 7 mm long and clearly primary magmatic grains, are aligned parallel with the ductile fabric. One of these megacrysts is zoned with respect to plagioclase feldspar exsolutions. This crystal has abundant exsolutions in a well-defined tabular core and a thin exsolution-rich zone in the otherwise homogeneous rim. Plagioclase feldspar is strongly stained. Dark minerals, mainly pseudomorphs after biotite, are chlorite and opaques. Muscovite occurs in sparse amounts in these pseudomorphs.

Along the vugs, the feldspars are clearly embayed (i.e. resorbed) and fringed by thin rims. The thin rims are made up of very fine-grained, colourless minerals and a dark, opaque-looking inner border with dusty appearance that is probably a dense staining composed of hematite. Secondary quartz is rare; only a few idiomorphic quartz crystals occur in the vugs. Some of these quartz crystals are coated by fine-grained rims that consist of colourless minerals with inclusions of tiny, flaky dark minerals (locally with greenish tints, probably chlorite) and opaques (locally with reddish tints, probably hematite). This is different from the other samples studied (e.g. C1, D1, D2 and D3), where the relationships are the reverse, i.e. idiomorphic quartz overgrows fine fringes.

D) Strongly altered rocks with vugs

D1: Sample level 295.82–295.89. *Very porous, strongly altered, red, medium-grained*

The thin-section has been cut perpendicular to the lineation. The metagranite is strongly altered with a partial loss of coherence. It is rich in vugs and relatively poor in quartz. Plagioclase feldspar is stained. Dark minerals are opaque-looking and largely fibrous. In most places, these minerals are intergrown with chlorite and are clearly pseudomorphs after biotite. Along the vugs, most feldspar grains have clear rims and sharp crystal faces, although some grains show embayments. Along some vugs, a thin rim of secondary, very fine-grained, colourless minerals occur. The inner part of this rim, along the contact to the matrix feldspar, is marked by minute brownish inclusions. Locally, opaque-looking minerals and/or radial aggregates of chlorite are present in the vugs. Some of the cavities are filled with quartz. This late-stage quartz is distinctly strain-free with straight grain-boundaries, and encloses the thin fringes of colourless minerals.

D2: Sample level 295.82–295.89. *Very porous, strongly altered, red, medium-grained metagranite.*

This sample has been taken at the same depth as sample D1, but the thin-section has been cut roughly parallel to the lineation.

D3: Sample level 290.25–290.28. *Strongly altered, porous, red, medium-grained, metagranite with a distinctive mineral foliation.*

The thin-section from this sample has been cut perpendicular to the planar and parallel to the linear, ductile deformational fabric. Sample D3 is similar to both D1 and D2 (5.6 cm beneath D3) but shows a stronger ductile deformational fabric. The distinctive foliation is developed along the contact to an amphibolite layer at 289.85–290.10 m (sample B2 above).

Appendix B

X-ray diffractograms

Sample level 256.10–256.39. *Sample from vugs in medium-grained metagranite.*

The sample from this level has been analysed in two ways: 1) the whole sample with a random orientation of mineral grains, and 2) the fine-grained fraction in the sample with a preferred orientation of mineral grains. In the X-ray diffractogram of the whole sample with random orientation, strong peaks mainly from hematite and plagioclase feldspar (albite) are shown. In the X-ray diffractogram of the fine-grained material with oriented mineral grains (scan from 2° to 35°, 2-theta), distinctive peaks from several other minerals are present. The hematite peak at 33.1° (2-theta) is the strongest one in the diagram. In addition, peaks from chlorite, biotite, plagioclase feldspar (albite) and possible anatase and rutile are present.

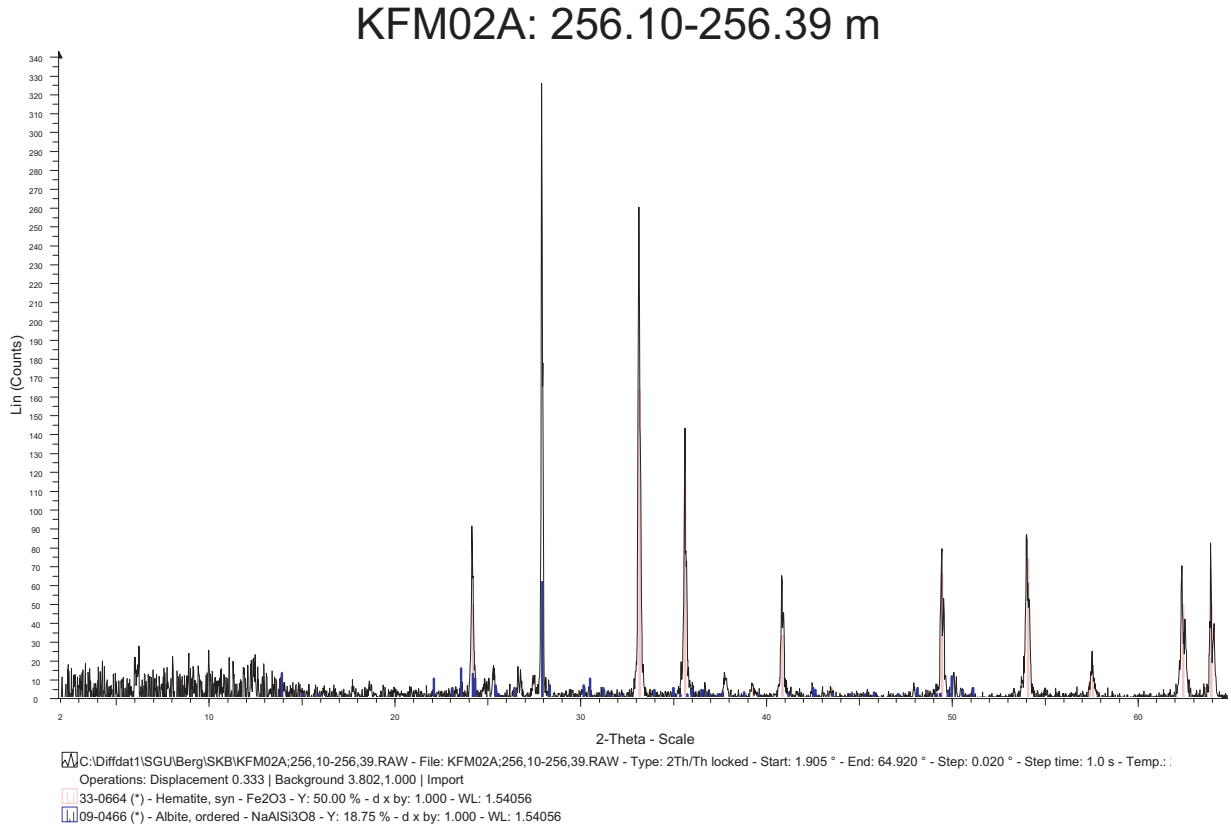

KFM02A: 256.10-256.39 m (oriented)

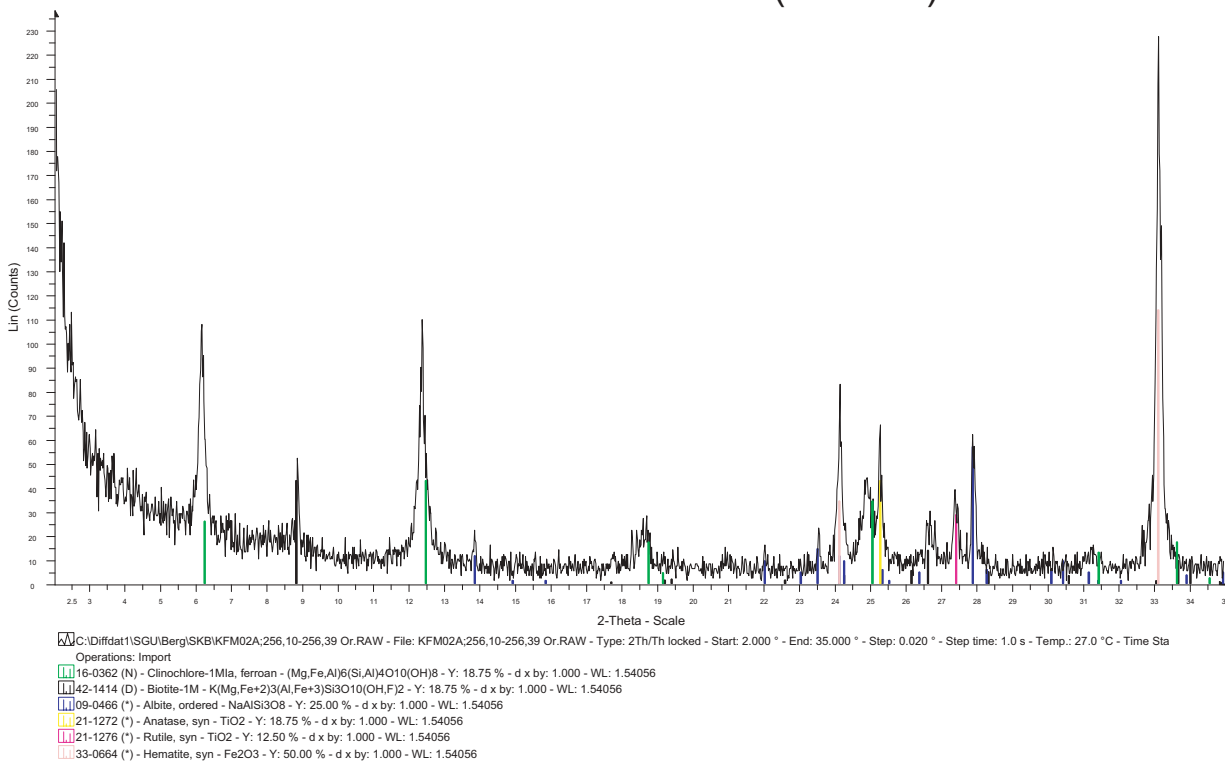

C:\Diffdat1\SGU\Berg\SKB\KFM02A;256,10-256,39 Or.RAW - File: KFM02A;256,10-256,39 Or.RAW - Type: 2Th/Th locked - Start: 2.000 ° - End: 35.000 ° - Step: 0.020 ° - Step time: 1.0 s - Temp.: 27.0 °C - Time Sta
Operations: Import
16-0362 (N) - Clinochlore-1MIa, ferroan - (Mg,Fe,Al)6(Si,Al)4O10(OH)8 - Y: 18.75 % - d x by: 1.000 - WL: 1.54056
42-1414 (D) - Biotite-1M - K(Mg,Fe+2)3(Al,Fe+3)Si3O10(OH,F)2 - Y: 18.75 % - d x by: 1.000 - WL: 1.54056
09-0466 (*) - Albite, ordered - NaAlSi3O8 - Y: 25.00 % - d x by: 1.000 - WL: 1.54056
21-1272 (*) - Anatase, syn - TiO2 - Y: 18.75 % - d x by: 1.000 - WL: 1.54056
21-1276 (*) - Rutile, syn - TiO2 - Y: 12.50 % - d x by: 1.000 - WL: 1.54056
33-0664 (*) - Hematite, syn - Fe2O3 - Y: 50.00 % - d x by: 1.000 - WL: 1.54056

Sample level 262.20–262.21. *Sample from vugs in medium-grained metagranite.*

The sample from this level is taken from a 10 mm large mineral aggregate. The aggregate is composed of dark-coloured crystals (mm-size). Material from the aggregate has been analysed with a random orientation of mineral grains. The X-ray diffractogram only shows peaks from hematite.

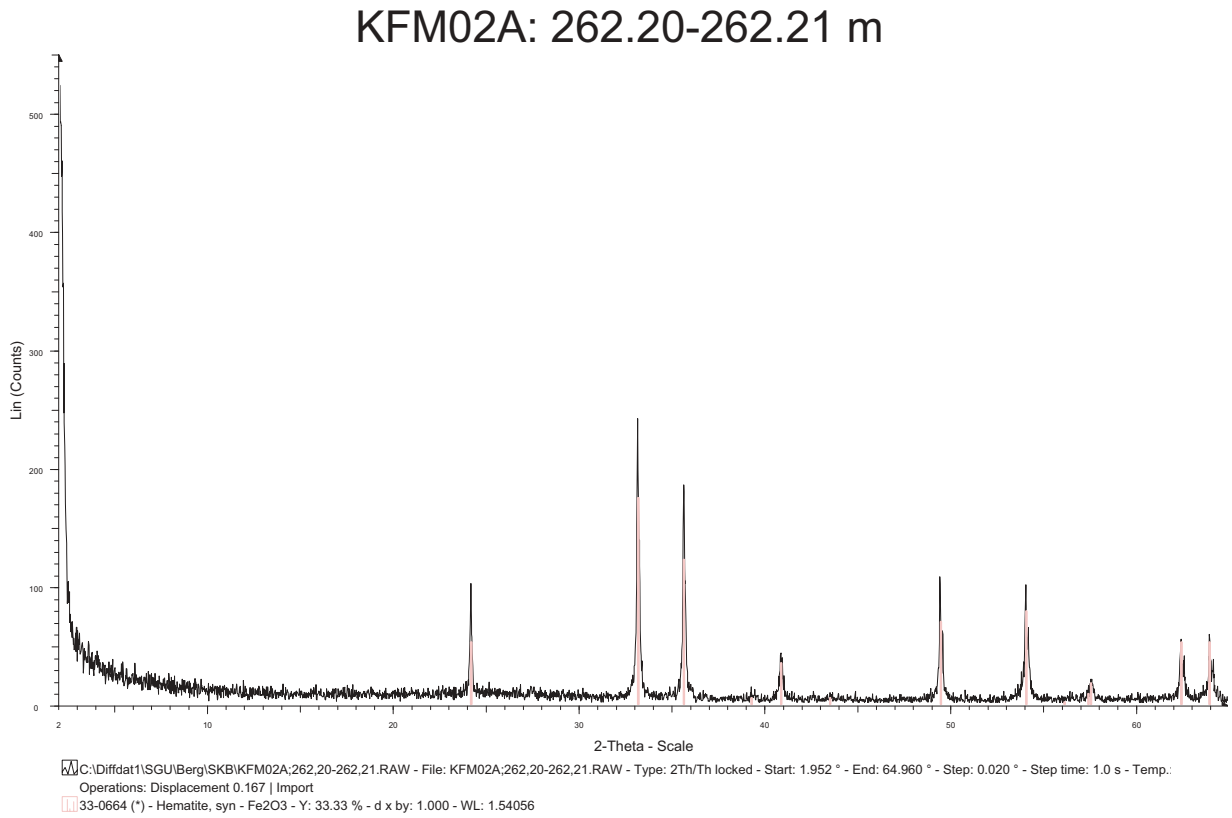

Sample level 270.10. *Sample from vugs in medium-grained metagranite.*

A green-coloured material has been analysed with a random orientation of mineral grains. The sample is composed of plagioclase feldspar (albite), quartz, chlorite and a small amount of hematite.

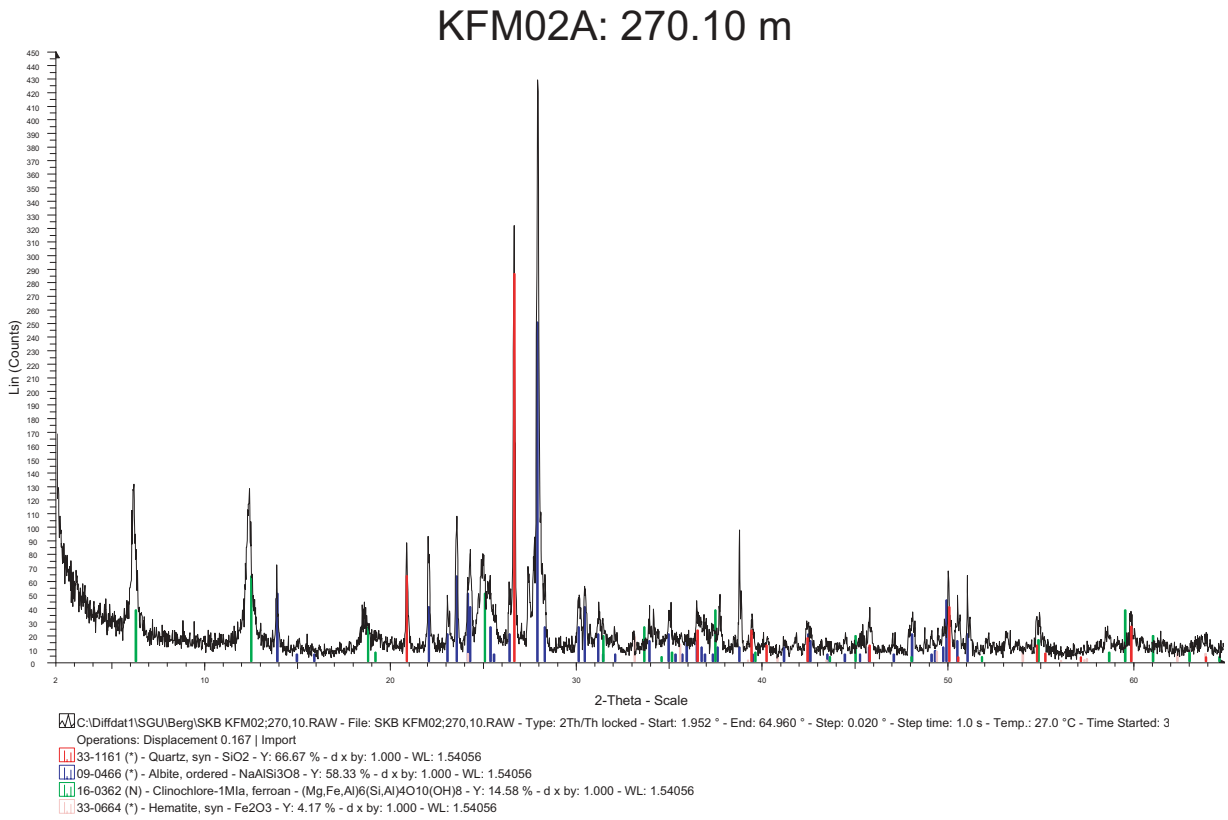

Sample level 275.20. *Sample from vugs in medium-grained metagranite.*

The sample from this level has been analysed in two ways: 1) the whole sample and 2) the fine-grained fraction in the sample with a preferred orientation of mineral grains. The X-ray diffractogram of the whole sample displays strong peaks, mainly from K-feldspar, quartz, plagioclase feldspar (albite) and chlorite, and small peaks from hematite.

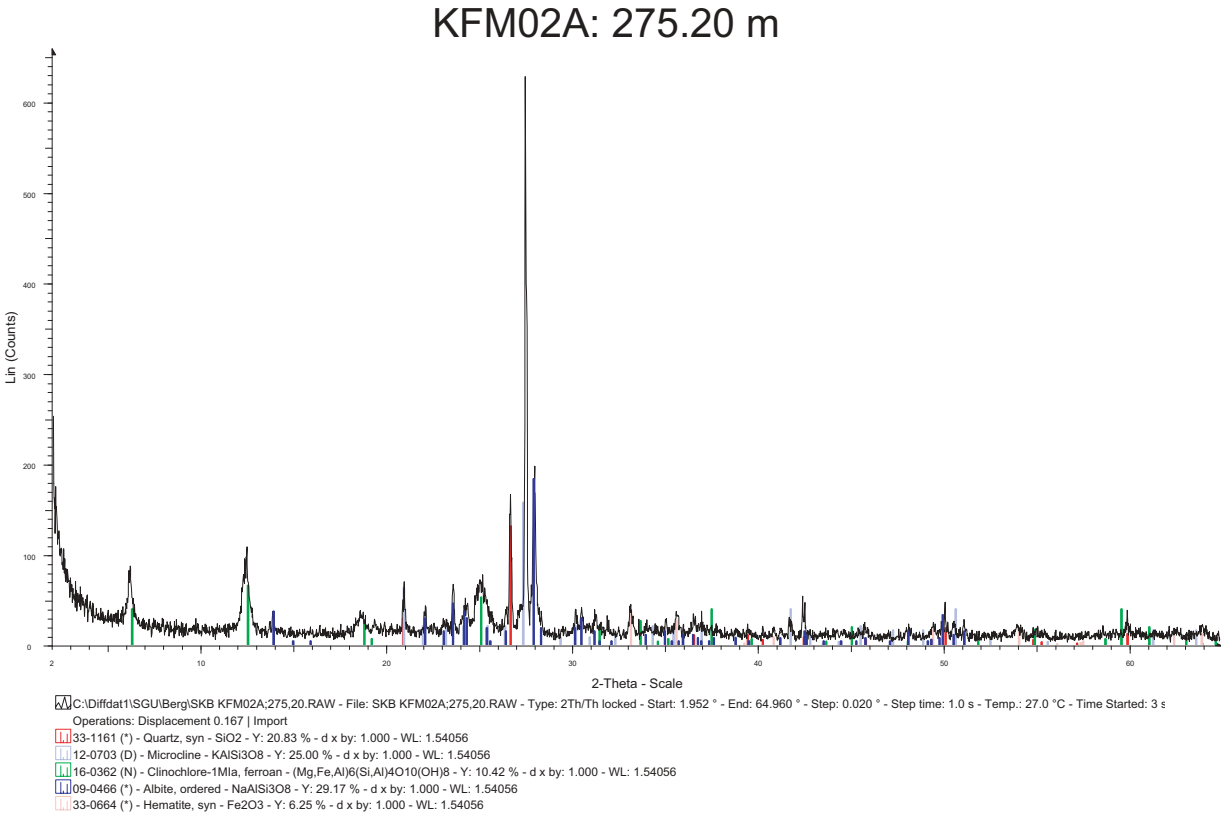

2) The fine-grained fraction was analysed in three ways; naturally, after saturation with ethylene glycol (EG-saturation), and after heating to 450°C for 2 hours. The analyses were performed with oriented mineral grains. For this reason, the 00l-peaks (basal spacings) from phyllosilicates are magnified, in this case the chlorite 001-, 002-, 003- and 004-peaks at 6.2°, 12.4°, 18.7° and 25.0° (2-theta), respectively. Neither the EG-saturation nor the heating changed the spacing of the chlorite. In comparison with the whole sample, the fine-grained material is richer in chlorite and poorer in, especially, K-feldspar.

KFM02A: 275.20 m (oriented)

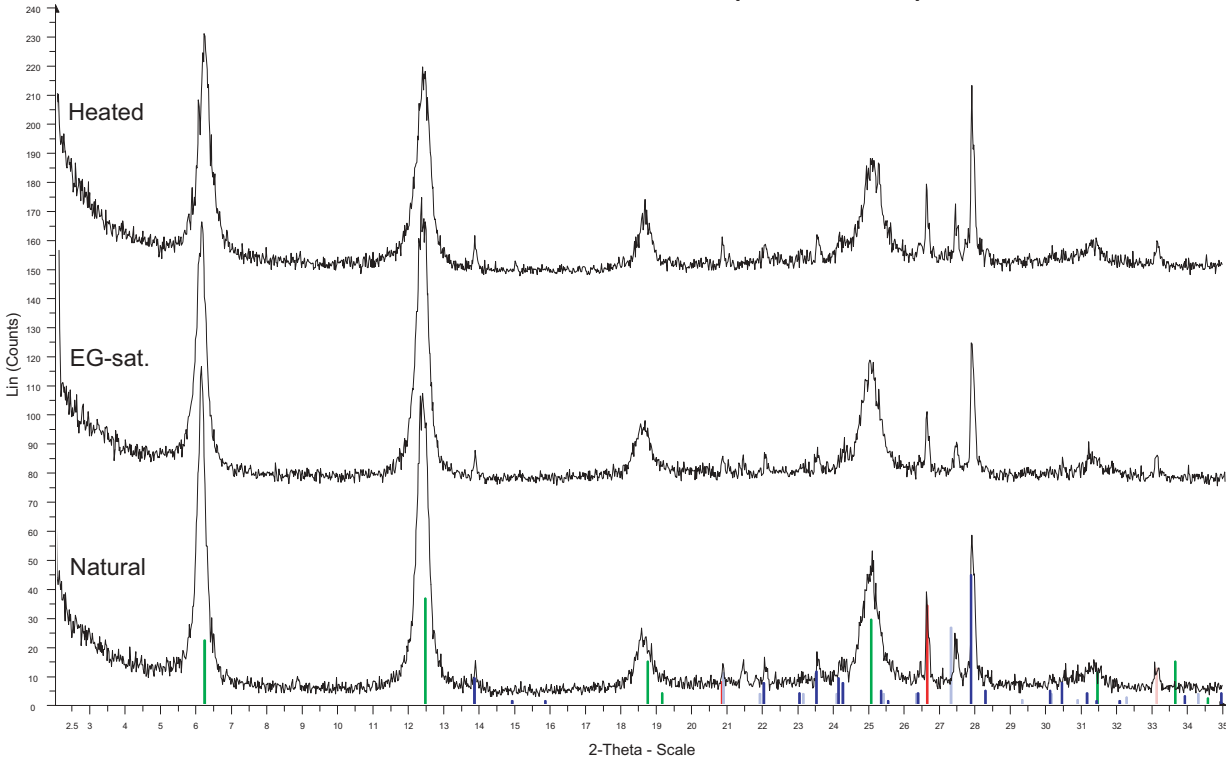

C:\Diffdat1\SGU\Berg\KFM02A;275,20 Sed.RAW - File: KFM02A;275,20 Sed.RAW - T
Operations: Y Scale 0.500 | Y Scale 0.500 | Import
Y + 40.0 mm - C:\Diffdat1\SGU\Berg\SKB KFM02A;275,20 SedEG.RAW - File: SKB K
Operations: Y Scale 0.500 | Y Scale 0.500 | Displacement -0.333 | Import
Y + 80.0 mm - C:\Diffdat1\SGU\Berg\SKB KFM02A;275,20 Sed 450 Deg.RAW - File: S
Operations: Y Scale 0.500 | Y Scale 0.500 | Import
33-1161 (*) - Quartz, syn - SiO2 - Y: 29.17 % - d x by: 1.000 - WL: 1.54056
12-0703 (D) - Microcline - KAlSi3O8 - Y: 22.57 % - d x by: 1.000 - WL: 1.54056
16-0362 (N) - Clinochlore-1MIa, ferroan - (Mg,Fe,Al)6(Si,Al)4O10(OH)8 - Y: 31.25 % -
09-0466 (*) - Albite, ordered - NaAlSi3O8 - Y: 38.19 % - d x by: 1.000 - WL: 1.54056
33-0664 (*) - Hematite, syn - Fe2O3 - Y: 10.41 % - d x by: 1.000 - WL: 1.54056

Sample level 278.19–278.23. *Sample from vugs in medium-grained metagranite.*

Some of the small vugs in the metagranite at this level are filled with dark, minute mineral grains. In order to collect a sample for analysis, material from the vugs was extracted with a dental drill. Analysis of this material demonstrates the difficulties encountered to obtain a pure sample of the dark mineral. As shown in the diagram, the material picked out contains quartz and alkali feldspars. The dark mineral is probably hematite.

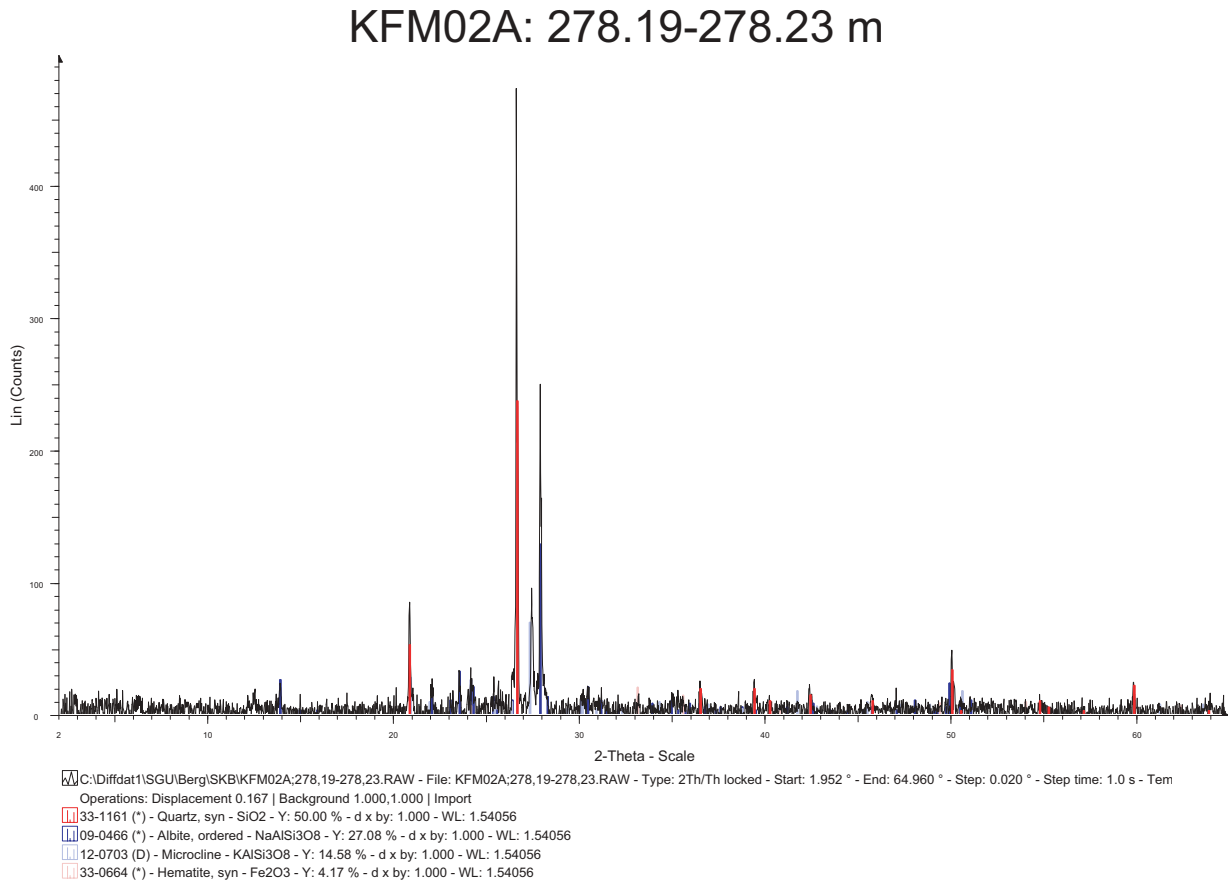

Sample level 283.73–283.75. *Sample from vugs in medium-grained metagranite.*

Fine-grained material extracted from the wall of the vugs in the metagranite has been analysed with a preferred orientation of the mineral grains. The material is mainly composed of chlorite and hematite. Smaller amounts of a mica-type mineral is also present, here tentatively interpreted as an illite.

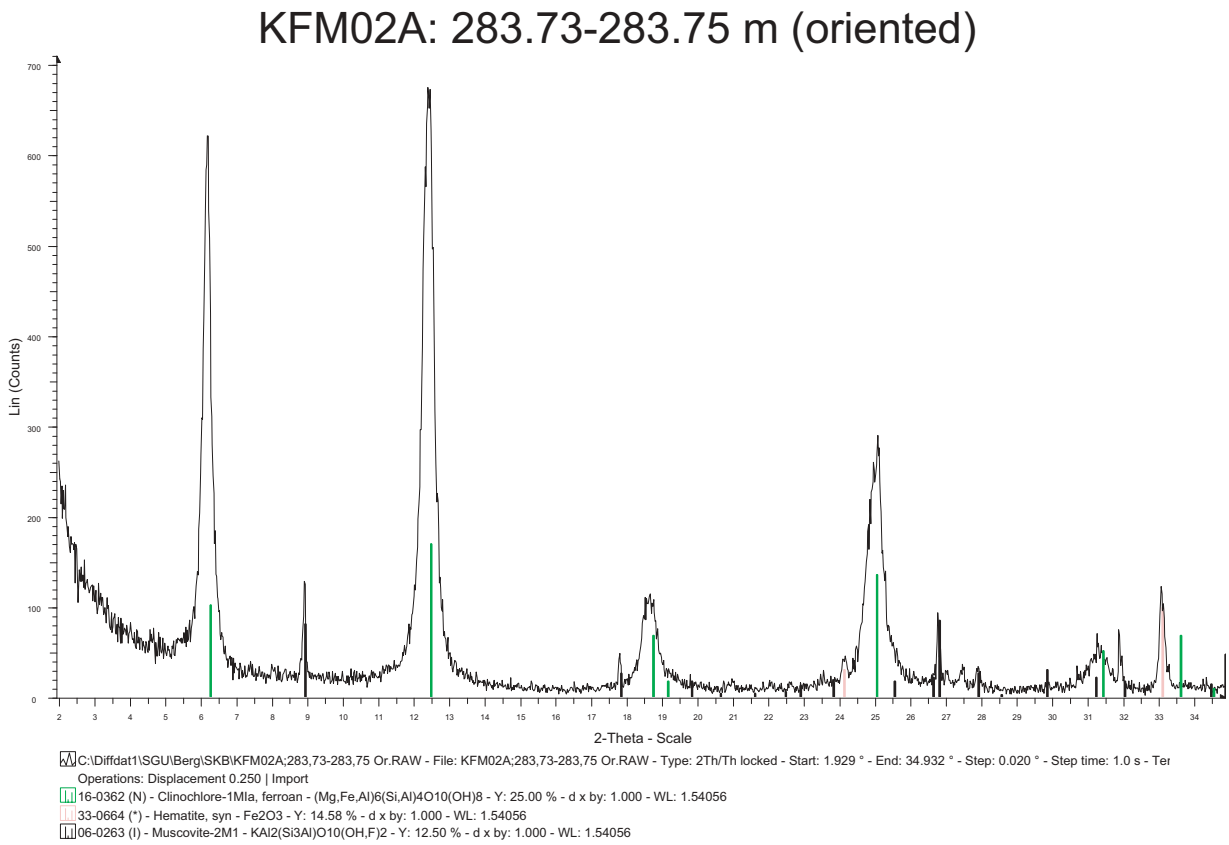

Sample level 288.12–288.17. *Small segregation of white-coloured material.*

A segregation of white-coloured material in the metagranite has been analysed. The white material consists of pure calcite.

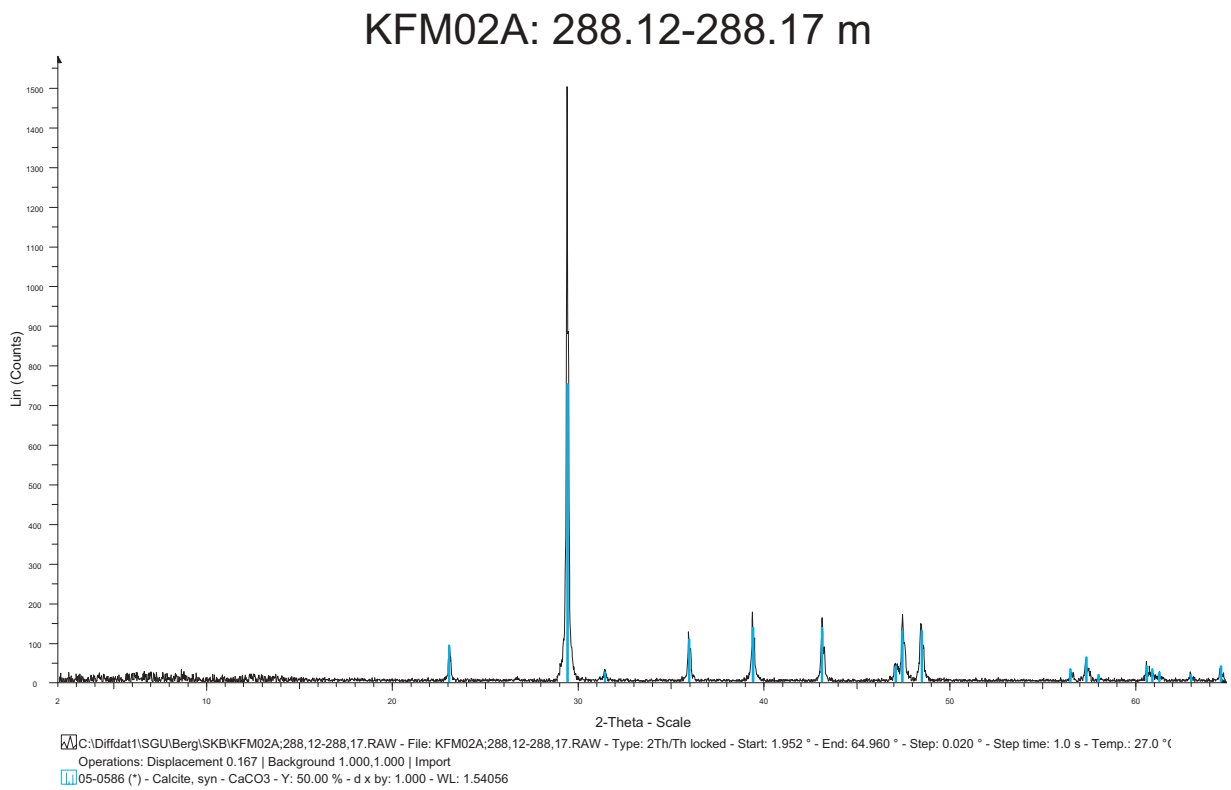

Sample level 289.37. *Sample from vugs in pegmatite.*

Material extracted from the wall of the vugs in the pegmatite has been analysed in two ways: 1) all the material 2) the fine-grained fraction with a preferred orientation of mineral grains. The mineralogical composition of the two fractions was very similar and only the X-ray diffractogram generated for all the material is shown. The material is composed of quartz, K-feldspar, plagioclase feldspar (albite), hematite and minor chlorite.

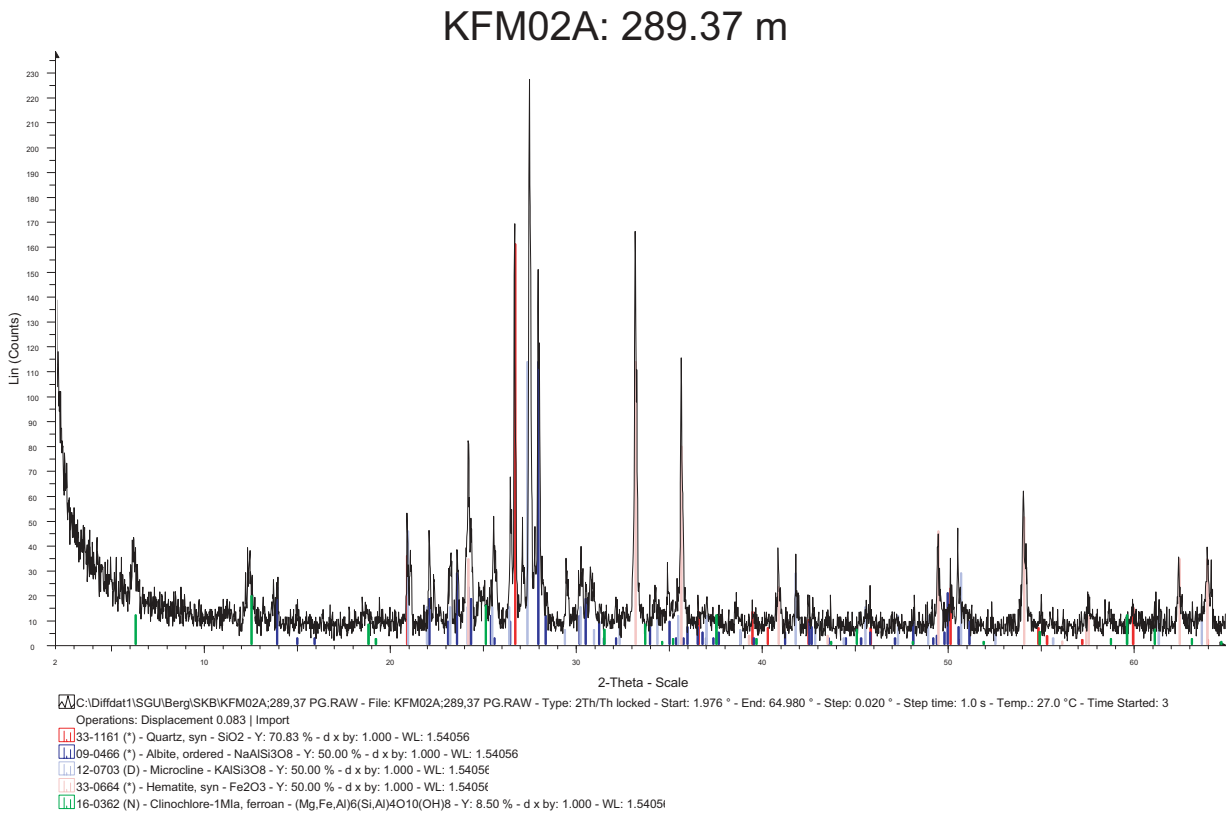

Sample level 290.03. *Altered amphibolite.*

This sample was taken from an altered, fine-grained amphibolite. The rock was ground and analysed with a random orientation of mineral grains. The XRD analysis shows that this rock is dominated by plagioclase feldspar (albite) and chlorite. Hematite, quartz and small amounts of a mica mineral (here interpreted as an illite) are also present in the rock.

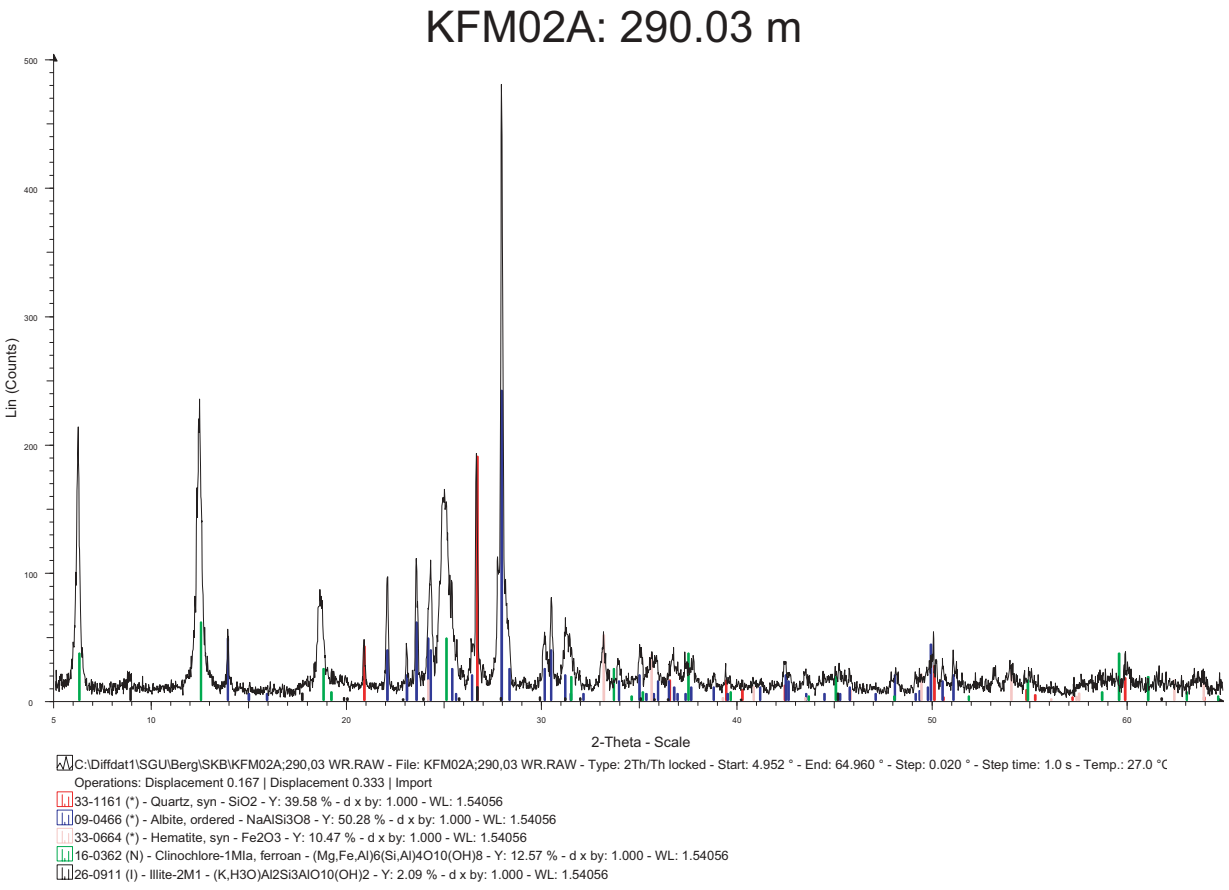

Sample level 291.17. *Fine-grained material associated with amphibolite in a segment of the core that has lost its coherence.*

This sample consists of dark brown, clay-like material. It occurs in a segment of the core which is dominated by amphibolite and which has lost its coherence. The material was analysed with a preferred orientation of mineral grains (scan from 2° to 35°, 2-theta). The material consists more or less entirely of chlorite. Small amounts of plagioclase feldspar (albite), illite and hematite have also been detected. The sample was also run after saturation with ethylene glycol and after heating to 450°C. No change of spacing in the chlorite lattice could be observed (cf sample from level 275.20 m).

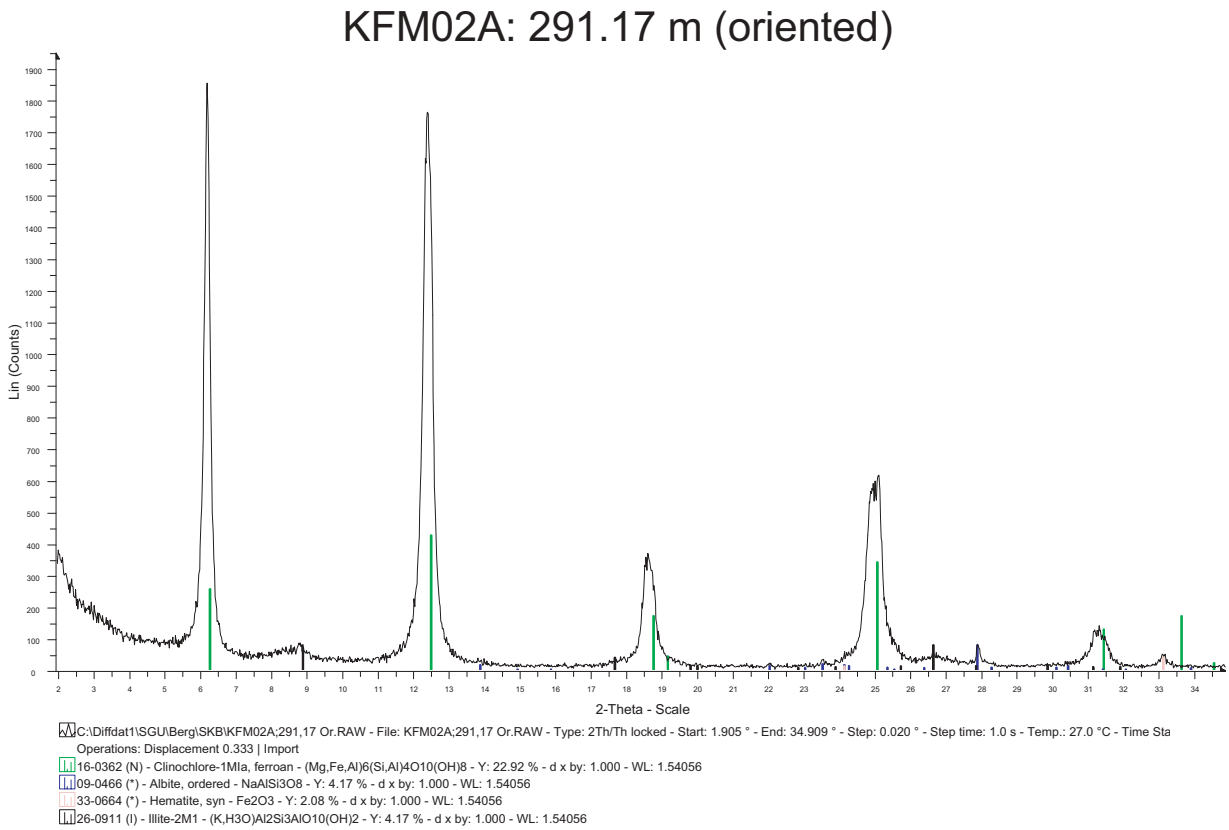

Sample level 294.59. *Fine-grained material (c 1 cm thick) along a fracture which separates amphibolite and strongly altered, medium-grained metagranite.*

Fine-grained, reddish brown material along a fracture which separates amphibolite and strongly altered and porous metagranite was extracted for analysis at this level. The sample was analysed with a preferred orientation of mineral grains (scan from 2° to 35°, 2-theta). Chlorite, plagioclase feldspar (albite) and hematite have been identified in the X-ray diffractogram. Rutile is also present in the sample.

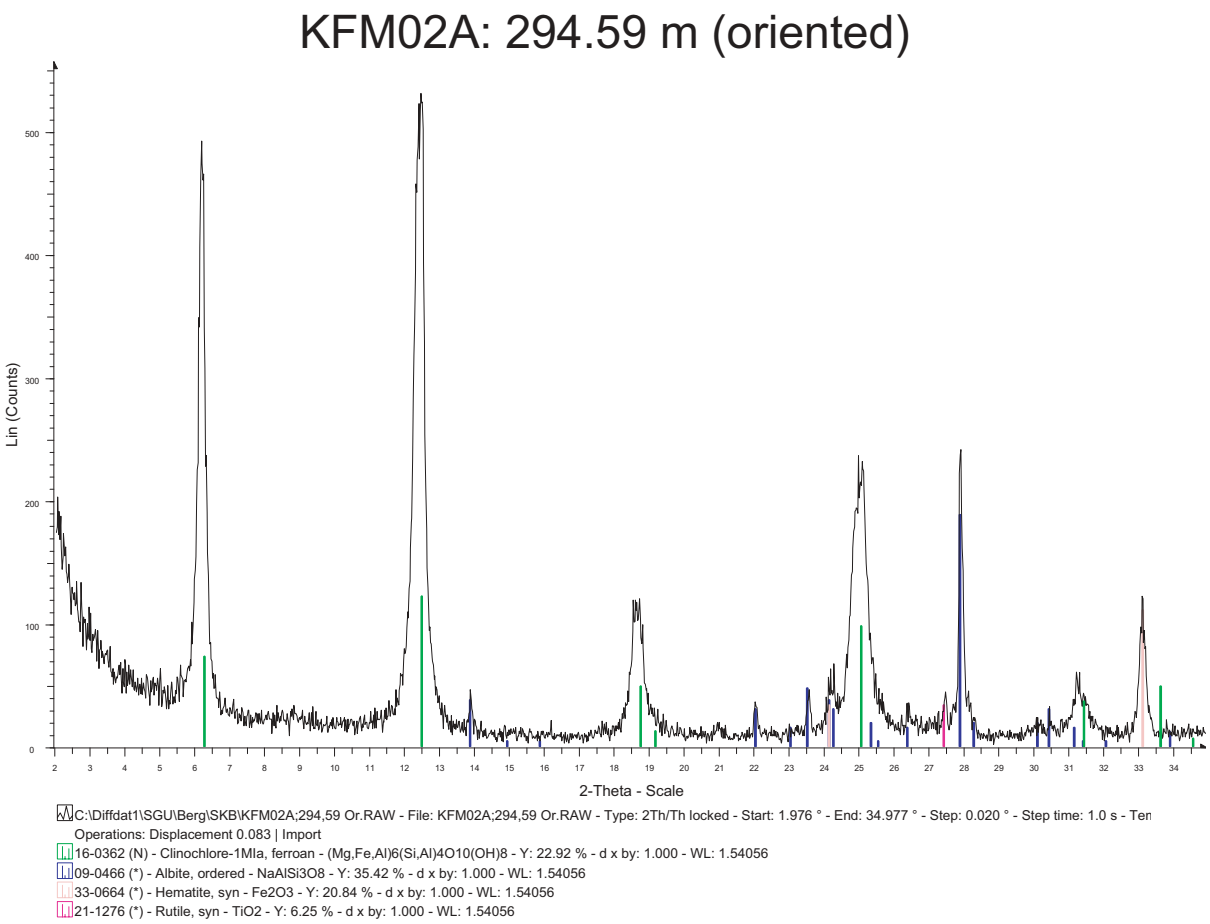

Sample level 295.56. *Sample from vugs in medium-grained metagranite.*

Fine-grained material extracted from the wall of the vugs in the metagranite has been analysed with a preferred orientation of mineral grains. In the X-ray diffractogram, only chlorite and hematite have been identified.